GKSS
FORSCHUNGSZENTRUM
in der HELMHOLTZ GEMEINSCHAFT

ETM format for creep deformation parameters

Authors:

J. D. Landes

K.-H. Schwalbe

W. Dietzel

ETM format for creep deformation parameters

Authors:

J. D. Landes

**(University of Tennessee,
Knoxville, TN, USA)**

K.-H. Schwalbe
W. Dietzel

**(Institute for Materials Research,
GKSS, Geesthacht, Germany)**

ETM format for creep deformation parameters

John D. Landes, Karl-Heinz Schwalbe and Wolfgang Dietzel

56 pages with 25 figures and 2 tables

Abstract

Parameters for the correlation of creep deformation and crack extension behavior are developed from principles that assume the commonality of all deformation forms. An assumption is made that the relationship between the force, crack length and deformation parameters has a separated format that is common for of all types of deformation. This allows the use of parameter forms developed for elasticity and plasticity to be extended to the characterization of creep deformation. Equation forms are developed based on the parameters C^*, C_t and on the δ_5 formats. These equation forms are needed to complete a procedure for predicting residual life in structural components with crack-like defects that operate in the high temperature creep deformation regime.

The formats proposed for some of these parameters were subjected to experimental evaluation. The evaluation was conducted with a Mg alloy, AZ31, which exhibited creep behavior at 150 °C. Both smooth tensile specimens and notched and precracked fracture mechanics specimens were tested. The results showed that the separation form of the equation appears to be experimentally validated.

ETM-Format für Parameter zur Beschreibung von Kriechverformungen

Zusammenfassung

Für Verformungen und Risswachstum im Kriechbereich werden Parameter entwickelt, wobei vorausgesetzt wird, dass die Beziehungen zwischen angelegter Kraft, Risslänge und Verformungsparametern für alle Verformungsarten von gleicher Form sind. Dies erlaubt die Übertragung von Zusammenhängen, die für linear elastisches und elastisch-plastisches Verhalten entwickelt wurden, auf den Kriechbereich. Ausgehend von dieser Überlegung werden für die Parameter C^*, C_t und δ_5 die entsprechenden Gleichungen hergeleitet, die für eine Prozedur zur Ermittlung der Lebensdauer riss-behafteter Komponenten unter Kriechbedingungen benötigt werden.

Die vorgeschlagenen Beziehungen werden experimentell anhand der Magnesium-Legierung AZ31 bei 150 °C verifiziert. Es werden sowohl gewöhnliche Zugproben als auch Bruchmechenikproben getestet. Die Ergebnisse bestätigen die gemachte Voraussetzung.

CONTENTS

KEYWORDS: Creep, Creep deformation, creep cracking, ETM, CTOD-δ_5, C*-parameter, C_t parameter

NOMENCLATURE

a   - crack length

a_{eff} - effective crack length

a_f - final crack length

a_o - initial crack length

A - coefficient in creep strain rate versus stress power law fit

b - uncracked ligament, W - a

B - specimen thickness

C(a/W) - Elastic compliance function

C*   - crack extension rate correlating parameter for extensive creep

C(t) - crack extension rate correlating parameter for small scale creep

C_t - crack extension rate correlating parameter for all creep ranges

$(C_t)_{SSC}$ - value of C_t for small scale creep

ds   - increment of integration for the C* integral definition

E   - elastic modulus

E′   - effective elastic modulus;
(E′ = E for plane stress, $E/(1 - v^2)$ for plane strain)

f(a/W) - geometry function in the K solution, $K = Ff/B\sqrt{W}$ formulation

f′   - derivative of f(a/W) with respect to a/W

F - applied load or force

F_{OC} - calibration force in extensive creep law using $\dot{\delta}_5$

F_Y - yield force, calibration in the δ_5 formulation

F_{cr} - constant in the determination of creep zone size;
(F_{cr} = 0.6 for plane stress and 0.3 for plane strain)

h_1 - factor in the C* handbook estimation formula

J - J integral

k - coefficient in the power law relationship between stress and strain

K - crack-tip stress intensity factor

K_{eff} - effective K modified with a plastic zone or creep zone crack extension

$\dot{K}_{eff}$ - time derivative of K_{eff}

m - constant in the essentially elastic δ_5 formula,
(m = 1 for plane stress and 2 for plane strain)

n - exponent in creep strain rate versus stress power law fit

N - exponent in the power law relationship between stress and plastic strain

r_c - creep zone dimension

$\dot{r}_c$ - time derivative of r_c

t - time

t_T - transition time between small scale creep and extensive creep

T_i - traction vector used in integral formulation of C*

$\dot{u}_i$ - displacement rate vector used in integral formulation of C*

U* - energy rate, area under a force versus deflection rate curve

U_t^* - time dependent value of U* in the small scale creep regime

v   - total displacement

v_{el} - elastic component of displacement

v_{pl} - plastic component of displacement

$\dot{V}_c$ - creep component of deflection rate

W - specimen width

W* - strain energy density rate in integral formulation of C*

x   - horizontal coordinate

y   - vertical coordinate

α   - factor in the crack-tip creep deformation zone, r_c

$α_n$ - factor in the evaluation of α;

   ($α_n^{n+1}$ is taken as 0.69)

β   - factor indicating how much of the creep zone, r_c, is contributing to
       effective crack advance, (β is usually taken as 1/3)

$β_1$ - Factor in the formulation of $δ_5$ for essentially elastic behavior;

   ($β_1$ = 2.41 for plane stress and 2.09 for plane strain)

$δ_5$ - crack tip opening displacement defined for a gauge length of 5 mm

$\dot{δ}_5$ - time rate of $δ_5$, used as a crack extension rate correlating parameter

$\dot{δ}_5$ * - $\dot{δ}_5$ for extensive creep

$\dot{δ}_{5OC}$ - a calibration value of $\dot{δ}_5$ used in the formulation of $\dot{δ}_5$ *

$\dot{\delta}_{5SSC}$ - small scale creep value of $\dot{\delta}_5$

ε - strain

$\dot{\varepsilon}$ - strain rate, time derivative of ε

γ - factor used in the handbook formulation of C*

Γ - integration path for C*

η - coefficient in C* and J definitions

κ - coefficient in the concise formulation for K

$\lambda(a/W)$ - Normalized elastic compliance, BEv/F

ν - Poisson's ratio

σ - stress

σ_{OC} - calibration stress in the creep formulation of $\dot{\delta}_5$ *

σ_Y - yield stress

Ω - Constraint factor used in the handbook formulation of C*

1 INTRODUCTION

Creep cracking parameters, those used to relate the creep deformation rate to crack-tip behavior, are used in a procedure for predicting residual life in structural components with crack-like defects that operate in the high temperature creep deformation regime, EFAM ETM-Creep 03 [1]. These parameters have traditionally been based on the parameters C* and C_t [2–4]. It is also desirable to develop creep deformation parameters for the Engineering Treatment Model format using the time rate of change of δ_5, $\dot{\delta}_5$ [5–7]. The δ_5 based parameters have the advantage that they can be easily measured on a specimen with a surface breaking defect and have no geometrical restrictions. However, the creep deformation parameters related to δ_5 have not been developed for structural component geometries. The same parameters are also used in a test procedure for determining creep crack extension rates, EFAM GTP-Creep 02 [8].

The forms for C* and C_t were developed by analogy to similar parameters used for plastic deformation behavior. This analogy depends on the ability to write a functional form relating force, displacement and crack length that separates and has a geometry function that is not dependent on the deformation process. In the past this has always been assumed but not experimentally verified.

In writing the δ_5 based relationhips this same format can be used to make inferences about the functiona form of $\dot{\delta}_5$ in the high temperature creep regime. The δ_5 parameter has an extensive set of formulations for both elasticity and plasticity. These have been developed for many structural component models. The ability to use these existing formulations to develop the δ_5 based parameters for creep deformation behavior would simplify the development of $\dot{\delta}_5$ forms. To use the analogies the same requirement for separation and functional independence of the deformation process is necessary. This is presently being studied with a set of creep deformation experiments and finite element analyses. The preliminary report of an experimental verification of these forms is included as part of this report.

The evaluation was conducted with a Mg alloy, AZ31, which exhibited creep behavior at 150 °C. Both smooth tensile specimens and notched and precracked fracture mechanics specimens were tested. The results are used first to look at the assumption that the format for writing these relationships does not depend on the deformation type, that is the forms are similar between, elastic, plastic and creep deformation. In addition the experimental results are used to look at some of the proposed parameter relationships. This work will be followed by additional experimental work as well as numerical work that will simulate the experimental program.

2 FRACTURE MECHANICS PARAMETER RELATIONSHIPS

Most of the fracture mechanics calibrations and relationships are written in formats that contain polynomials. This is done largely because the relationships among the parameters were developed numerically, resulting in tabular or graphical values but not functional relationships. Functional relationships are often more convenient to use than tabular data, for example, when a calculation program is needed for data reduction. To give the parameters functional relationships the tabular values were fitted with polynomials. The result is a form that is convenient to use in some cases but not necessarily in every case. The polynomial forms are easy to use in computational programs; however, when mathematical evaluations of the relationships are needed, the polynomial terms can cause difficulty because they are often too cumbersome to use in analytical relationships. Integration or differentiation of these polynomials can be difficult or impossible in closed form. In addition the polynomial fits give the user little idea of how the different parameters relate.

Examples of the parameter relationships that are usually expressed in polynomial forms are the following: i) the relationships between the crack-tip stress intensity factor, K, and crack length, a; ii) the relationships between specimen elastic compliance, v_{el}/F, and crack length; and iii) the relationships between a limit force, F_Y, and crack length. These relationships have been expressed in polynomial forms for most of the years that the fracture mechanics methodology has been in use and the users are accustomed to calculating the parameters from these polynomial formats. However, with these formats it is difficult to see and appreciate the relationships on which these parameters are based and the commonality that exists among them. Fracture mechanics relationships can be written in more concise forms due to the separability that exists among the fundamental relationships. Using the more fundamental relationships results in a format that is easier to use and makes better sense for understanding the relationship among the parameters.

To understand the commonality among relationships it is important to understand the fundamental parameters that control the structural loading system. A conventional analysis of a loaded system uses two fundamental parameters to describe the condition of the system. One is the loading parameter, that is in the form of an applied force, moment or stress and the second describes the deformation response which is a measure of displacement or rotation of the applied loading points or other significant points or a measure of strain. The relationship between, force and displacement (or stress and strain) defines the condition of the loaded structure. Using a parameter like force (stress), the information can be used to evaluate the failure possibilities of this structure. These variables can be substituted for by other similar parameters; for example, the force could be pressure and displacement could be diametral change in a pressure vessel analysis.

Fracture mechanics identifies an additional parameter that can influence structural behavior, that of a crack-like defect. It is often the influence of the crack that is the most important consideration relative to the failure potential of the structure. A conventional failure analysis, based solely on stress and strain parameters and ignoring the influence of the crack, can be in error. For a fracture mechanics analysis, the behavior of the crack, relative to a change in its length, gives an extra parameter to evaluate and also aids in making the analysis of failure more realistic. The fracture mechanics relationships then have three related parameters to consider. The force (or stress), displacement (or strain) and crack length. The relationship between the first two is given by constitutive equations that can be as simple as a unidirectional elastic relationship, or extremely complicated considering behaviors like plasticity, visco-elasticity and creep. However, these can be expressed in functional form where one parameter takes the role of the independent variable and the second the dependent variable. Given a force, (stress) the constitutive relationships predict the displacement (strain). For the fracture mechanics case, the added crack length parameter then gives two independent variables and the third dependent. However, the two independent variables are not actually independent and need an additional relationship to describe the complete behavior of the system. This is usually specified by some kind of fracture law based on a fourth parameter that is also a function of the three variables; force, displacement and crack length. The relationship of these three parameters can be further explored by considering the interactions of these system relationships when the system is subjected to an applied force.

3 SYSTEM RELATIONSHIPS

As stated above, the three fracture mechanics variables, force, F, displacement, v, and crack length, a, have two independent variables that are not truly independent. If the force on the system is changed there is usually an accompanying displacement change. However, the crack length may also change due to failure processes like unstable fracture or stable, ductile tearing, or also possibly due to subcritical crack extension processes like fatigue or creep crack extension. It would be convenient to be able to predict the crack length changes from one of the other two parameters, but unfortunately, crack length change is usually related to the other two variables in a somewhat complex manner. Therefore, a fourth variable is usually introduced to relate the two independent variables. Parameters like K, J and δ_5 can be used to characterize the conditions that cause the crack length to change.

The relationship between these three variables has been shown to be separable by

Ernst and Paris [9, 10]. Taking force, F as the dependent variable in the relationship

$$F = F(a,v) \tag{1}$$

separability allows the relationship to be written as

$$F = G^*(a/W) \text{x} H^*(v/W) \tag{2}$$

that is the separable function for F is two independent functions, $G^*(a/W)$ and $H^*(v/W)$, that are multiplied together. This separability is a tacit but fundamental assumption throughout the history of fracture parameter determination. For example the well known formula for J

$$J = \frac{\eta}{bB} \int F dv \tag{3}$$

is based on the separability of the functional relationships. This was first introduced by Rice et. al in their work to develop simple J formulas for different specimen type geometries [11].

Separablilty is schematically illustrated in Figure 1. Force versus displacement of a body with stationary cracks shows different values for identical bodies but with differing crack lengths, a/W, Fig. 1a. If the force is divided by the geometry function, $G^*(a/W)$, the different curves collapse onto a single curve, Fig. 1b. The original argument for this separability was developed from classical mechanics [12] and is analytically based. However, Sharobeam and Landes [13] used a scheme to test the separability condition for experimental data using a force ratio technique. With this they showed that separability is experimentally verified for most of the common specimen and structural geometries. They demonstrated this for systems using the plastic component of displacement, v_{pl}, as the argument of the H function, $v_{pl} = v -$ FxC(a/W), where C(a/W) is a compliance function that is usually specified for each geometry in the form of a polynomial fit. The term FxC is sometimes written as v_{el} so that $v_{pl} = v - v_{el}$. The separable form of the relationship between force, crack length and plastic displacement was written with all length terms being normalized by a constant length factor. This normalization factor was chosen, following the lead of Ernst et. al [10] as the specimen width, W. Therefore the separable relationship of Eq. (2) becomes
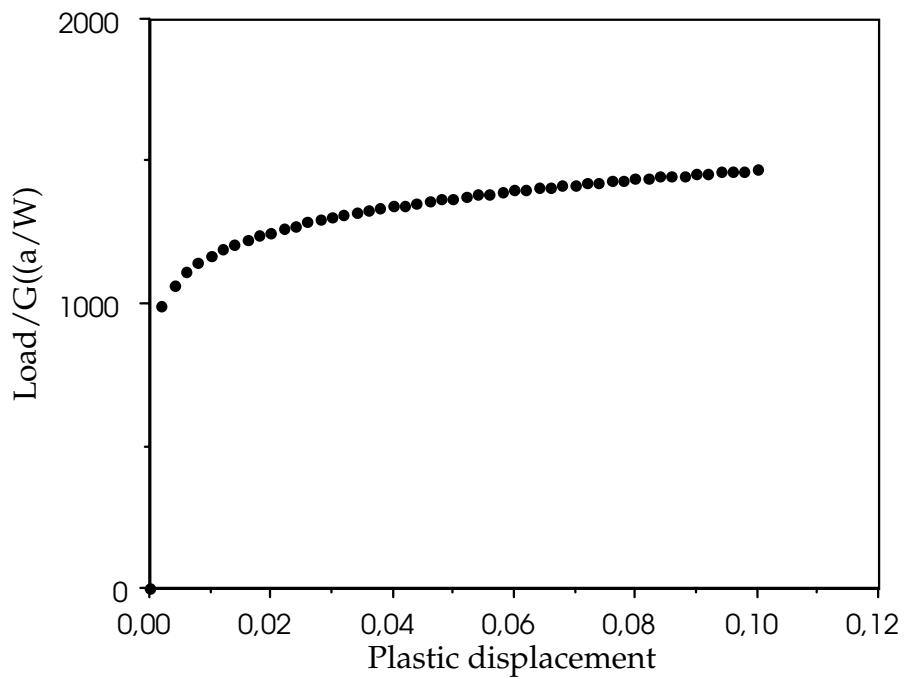
$$F = G^*(a/W) \text{x} H(v_{pl}/W) \tag{4}$$

or for convenience the crack length, a, is often replaced by an uncracked ligament length, b, where b = W – a. Therefore,

$$F = G(b/W) \text{x} H(v_{pl}/W) \tag{5}$$
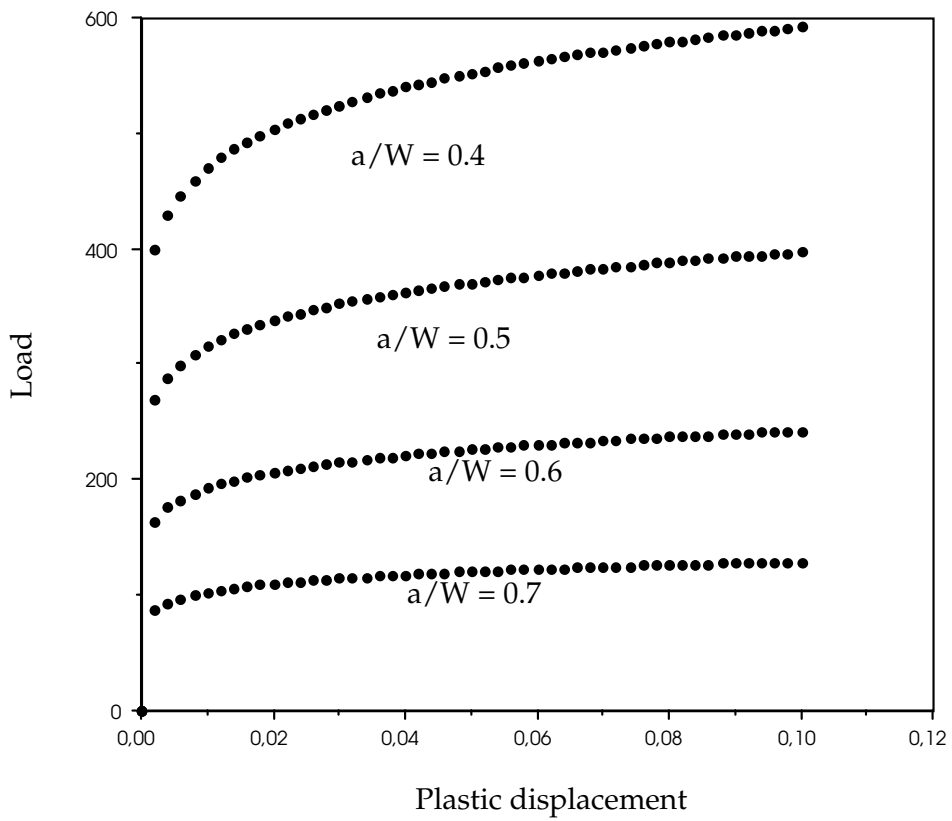
Figure 1a: Schematic of load versus plastic displacement.

Figure 1b: Schematic of normalized load versus plastic displacement.

The work of Sharobeam and Landes [13] further evaluated the G(b/W) function for many geometries and found that for most geometries the G function took the form

$$G(b/W) = BW(b/W)^{\eta} \tag{6}$$

where B is the specimen thickness and η is a term that is used in the calculation of J for Eq. (3). The form for the separable force function becomes

$$F = \{BW(b/W)^{\eta}\}\{H(v_{pl}/W)\} \tag{7}$$

This is a convenient form to work with in that the functional form of G is easy to determine from known calibration terms and the function H is the only one that needs to be determined to specify the relationship in Eq. (7). H can be determined from experimental work or numerical analysis. The H function could be determined from a test in which the crack length can be held constant, for example, a test of a blunt notched specimen that has a notch radius which is large enough to eliminate any crack extension but is still small enough to act as a crack-like defect.

Further work by Donoso and Landes [14] showed that the H function is basically determined by the stress-strain character of a material and H can be derived from a tensile test. This means that the two functions in the separable form of Eq. (5) are not difficult to determine.

4 PHILOSOPHY OF SEPARABILITY

The philosophy that is applied to the analogies made between plasticity and creep for the C* and C_t parameters is that the separated form of the force, displacement and crack length functions does not depend on the nature of the deformation function, H. That is the G function should be independent of the nature of the deformation. Until recently there was not enough data to study this for creep deformation but it can be compared for elastic and plastic deformation. The experimental demonstration of separability was done for the system of plastic deformation using force, F, plastic displacement v_{pl}, and ligament, b. A similar demonstration can be made for the system of elastic deformation by writing the compliance $v_{el}/F = C(a/W)$ or more commonly

$$BEv_{el}/F = \lambda(a/W) \tag{8}$$

or rearranging

$$F = \{BW/\lambda(a/W)\}\{Ev_{el}/W\} \tag{9}$$

Separability is already a part of that elastic relationship. The G function, $\{BW/\lambda(a/W)\}$, is the one that describes how the force depends on crack length whereas the H function, $\{Ev_{el}/W\}$, describes the elastic deformation behavior.

If the functions truly separate, the G function should not depend on the form of the H function. Therefore, the plastic and elastic deformation systems should give the same G function, although the H function is completely different. This should be true not only for elastic and plastic systems but also for all other types of deformation behavior including creep. An advantage of this is that the G function can be defined with a more convenient system and applied to others. For example, G could be defined for elastic or plastic deformation where the calibration functions may already exist and be applied to creep deformation.

One of the factors that could cause some problem for finding a G function that is compatible for all systems is that the system might be defined in different ways for the various types of behavior. For example, in comparing the plastic and elastic systems, the plasticity in most cracked geometries is confined to a smaller region like that of the uncracked ligament, the region between the crack tip and the nearest boundary. The elastic system, on the other hand, could be covering a much greater region, combining the uncracked ligament with the remaining parts of the structure to contribute to elastic behavior. Therefore, it is possible to have two different systems when defining the G function. Then a common G function might not be found for all conditions. However, when the systems are defined in a compatible way, the comparisons should work well. The parameters that are used in the classical fracture mechanics approach have been defined in other formats for both elastic and plastic systems. These can be used as an example to show that when the systems are compatible, a compatible G function can be observed.

The use of the separation philosophy to demonstrate the common origin of many of the fracture relationships is demonstrated in the next sections. For convenience two geometrical systems are used as examples, the compact specimen, C(T), Fig. 2a, and the single edge cracked tension geometry, SE(T) Fig. 2b. The former is exclusively a test specimen geometry and the calibration functions relating the parameters, F, v and a are well known for this geometry. The SE(T) geometry is more of a structural element model. Although it is not used as a fracture test specimen geometry, it also has the calibration functions developed. In addition the experimental evaluation of these forms was done for both of these geometries for plastic deformation by Sharobeam and Landes [13].
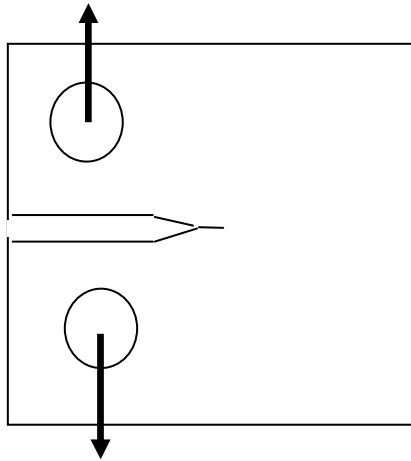
« Figure 2a:
Compact specimen
geometry, C(T).
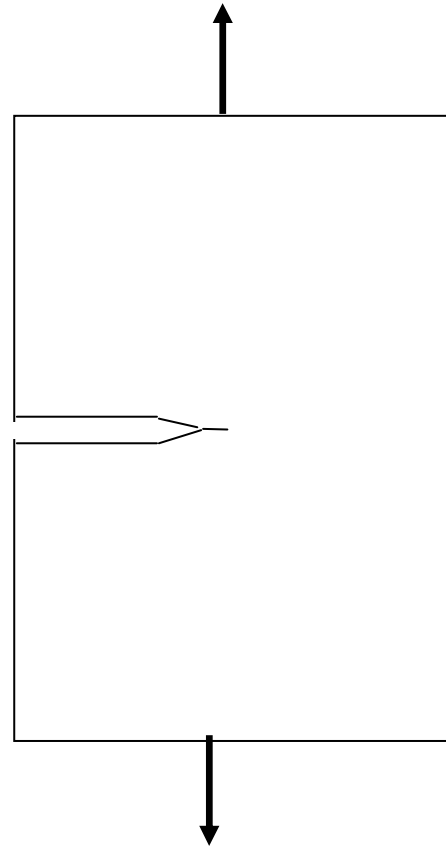
Figure 2b: »
Single edge cracked geometry, SE(T).

5 ELASTIC VERSUS PLASTIC CALIBRATIONS

The original forms for separation were developed from the relationship between force, crack length and plastic displacement. Sharobeam and Landes [13] looked at experimental tests of blunt notched specimens and suggested that the form of the G relationship is the one given in Eq. (6). The experimental results gave slightly different values of the exponent η than the ones that were used for the J calibration in Eq. (3). They found values that ranged from about 2.1 to 2.4 depending on the material hardening and found that η was virtually independent of crack length. The η for the J calibration used in test standards was based on a slipline field analysis followed by a curve fit of a straight line and had not been examined numerically. It had the form η = 2 + 0.522(b/W) which meant that it was a weak function of b/W. However the values of η in the a/W range used for testing are compatible with the one from the test standard [15].

Commonality of the G function for elasticity and plasticity means that the forms in Eqs. (7) and (9) should be identical. However, the compliance form of Eq. (9) has already been established for many geometries. Using the two examples mentioned previously, the C(T) for a specimen geometry and the SE(T) for a structural geometry, the relationship means that the compliance given by a simple function of

b/W should be identical to the polynomial. That is

$$F = BW(b/W)^{\eta} \, H(v_{el}/W) \; = [BW/\lambda(a/W)]x[Ev_{el}/W] \tag{10}$$

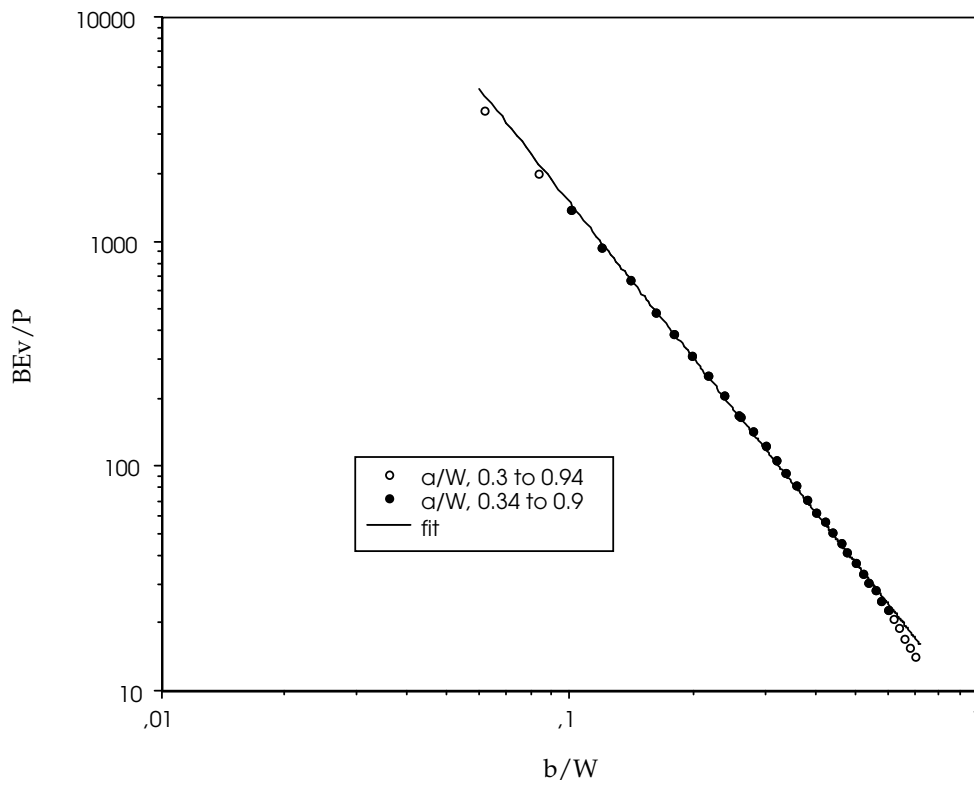Or using the polynomial format for $\lambda(a/W)$ in the C(T) specimen

$$\frac{BEv}{F} = \left[\frac{1+\dfrac{a}{W}}{1-\dfrac{a}{W}}\right]^{2}\left[\begin{array}{l}2.163 + 12.219\left(\dfrac{a}{W}\right) - 20.065\left(\dfrac{a}{W}\right)^{2} \\[2mm] -\,0.9925\left(\dfrac{a}{W}\right)^{3} + 20.609\left(\dfrac{a}{W}\right)^{4} - 9.9314\left(\dfrac{a}{W}\right)^{5}\end{array}\right]$$

$$= \frac{1}{\kappa\left(\dfrac{b}{W}\right)^{\eta}} \tag{11}$$

where κ is a constant that can be defined empirically from a fit of the polynomial form.
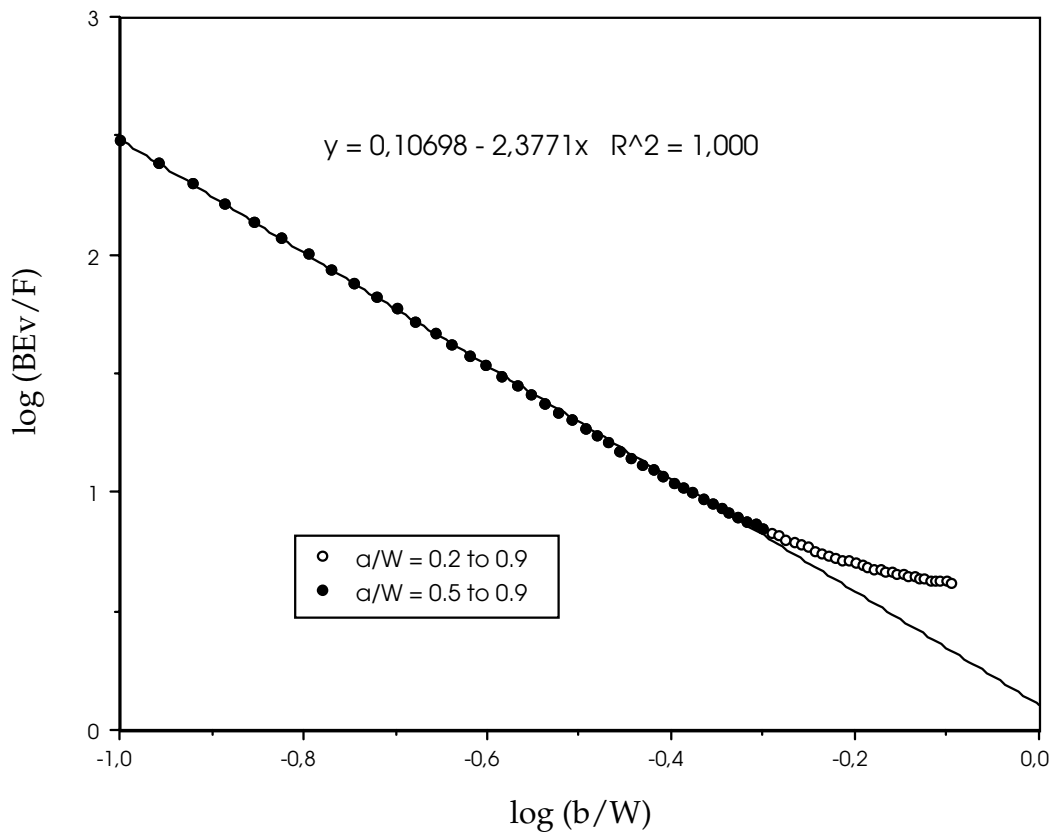
The relationship in Eq. (11) is compared in Figure 3a for the C(T) specimen geometry where the compliance polynomial is plotted as a function of b/W in log-log format. The fit to the data, solid points, shows that this relationship holds fairly well over a range of a/W going from 0.4 to 0.9, giving an η value of 2.285. Also, for this fit the intercept term gives a value of the constant κ as 0.1314. This is the range of a/W where the specimen is most used. However, when the limits are extended a little, the relationship between the compliance polynomial and b/W begins to take a slightly different form. In Fig. 3a the points deviate from the linear log-log fit, that is the power law relationship of Eq. (11), when the range of a/W is extended from the original 0.4 to 0.9 to a range going from 0.3 to 0.94, open points. This can be seen better in Figure 3b where the points are replotted as actual values on a log-log scale.
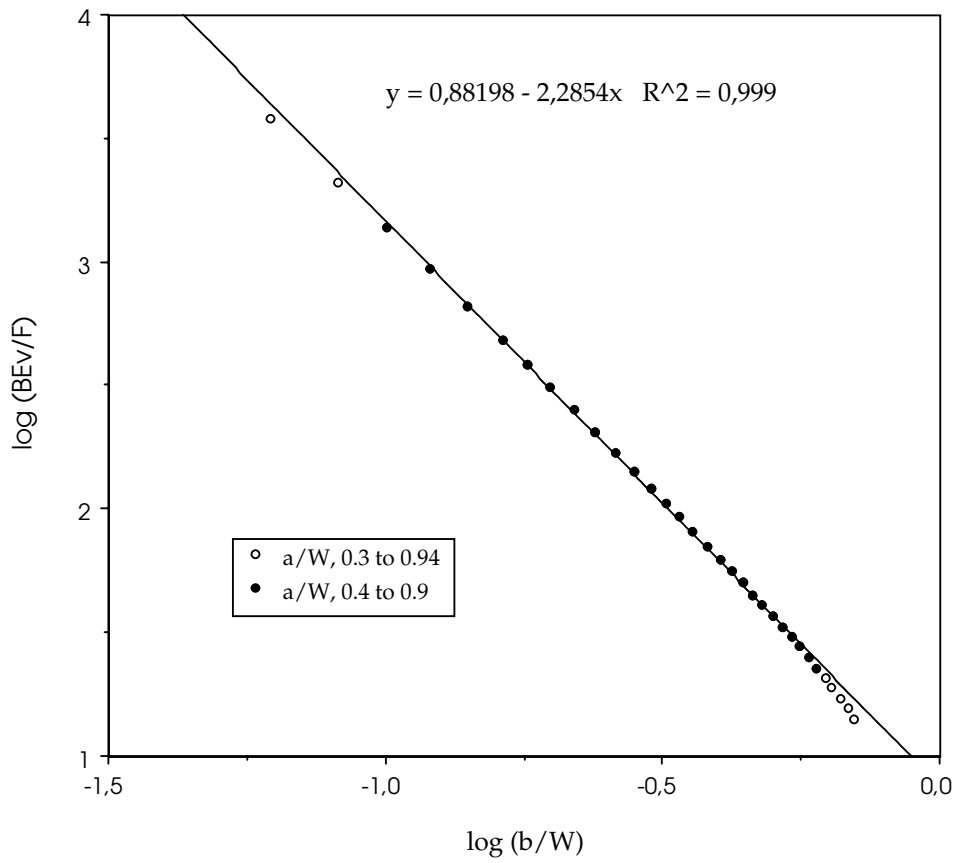
Figure 3a: Log-log plot of BEv/F for C(T) geometry.

Figure 3b: Plot of BEv/F vs b/W for C(T) geometry.

$y = 0,10698 - 2,3771x \quad R^2 = 1,000$

Legend:
○ a/W = 0.2 to 0.9
● a/W = 0.5 to 0.9

Axes: log (BEv/F) vs log (b/W)

Figure 4: Log-log plot of BEv/F for SE(T) geometry.

A similar format can be developed for the SE(T) geometry. This is done and is compared in Figure 4. Here the relationship fits the power law well for a/W between 0.5 and 0.9 with η being about 2.38. Again the points deviate from the linear fit when the range of a/W is extended to 0.2. The inability of the elastic and plastic functional forms to cover the entire a/W range could mean that the G function is not really independent of the deformation process. However, that assumption has been made in other systems and needs to hold or some of the existing fracture mechanics work may need to be reformulated. It is more likely that the suggestion made earlier that the elastic and plastic systems may not always be defined in a compatible way, that is over a common gage length, is a better explanation. For deeper cracks the predominant elastic deformation could be in the uncracked ligament region where plasticity is confined. For shorter cracks the elastic deformation could be spread over a larger area of the overall geometry whereas the plastic system which is confined to the ligament behind the crack. However, for very short cracks the plastic system also changes as gross yielding occurs and the plastic strains are not confined to the uncracked ligament behind the crack. In that case the separation relationship might no longer work for plasticity. These are reasons why the G function may not be similarly defined between elasticity and plasticity for all crack lengths and care should also be taken for other deformation systems.

6 FRACTURE MECHANICS EXPRESSIONS WITH A CONCISE FORMAT

The ability to write the compliance expression in a more concise form than the traditional polynomial, Eq. (11), gives an advantage in formulating the basic fracture mechanics relationships. Some simple applications of the concise form for the compliance function are in writing the expressions for K and limit force. A simple relationship exists between compliance and crack-tip stress intensity factor, K. This is given from the modification of the Griffith approach as

$$\frac{K^2}{E} = \frac{F^2}{2B}\frac{dC}{da}$$

(12)

Then using the form in Eq. (11)

$$K = \frac{F}{B\sqrt{W}} f\left(\frac{a}{W}\right) = \frac{F}{B\sqrt{W}} \left[\frac{\sqrt{\frac{\eta}{2\kappa}}}{(\frac{b}{W})^{\frac{\eta+1}{2}}} \right]$$

(13)

where η and κ have been previously defined. Comparing this f(a/W) to the usual polynomial form for the C(T) geometry gives

$$f(\frac{a}{W}) = \left[\frac{(2+\frac{a}{W})}{\left(1-\frac{a}{W}\right)^{\frac{3}{2}}} \right] \left(0.886 + 4.64\frac{a}{W} - 13.32(\frac{a}{W})^2 + 14.72(\frac{a}{W})^3 - 5.6(\frac{a}{W})^4 \right)$$

(14)

$$= \left[\frac{\sqrt{\frac{\eta}{2\kappa}}}{(\frac{b}{W})^{\frac{\eta+1}{2}}} \right]$$

A comparison of the two f(a(/W) functions, the traditional polynomial and the one represented by the concise form, is given in Figure 5. A similar expression to Eq. (14) can be developed for the SE(T) geometry. The comparison of this with the polynomial form of f(a/W) is given in Figure 6. The C(T) geometry shows a better

comparison but both are good over the ranges of a/W observed for good linear fit of the compliance forms in Figs. 3 and 4.

The use of a more concise form like the one in Eq. (13) can have advantages for some applications. The calculation of residual life for a fatigue crack extension case involves an integration with the K solution in the denominator of the integrand. This is very difficult in closed form for K solutions given in the form of a polynomial because the polynomial cannot be integrated. However, the concise form of K given in Eq. (13) can easily be integrated. Many other advantages of this format have been suggested [16, 17].

An additional relationship that can be taken in a more concise format is the limit force, F_Y. Taking the limit force as a calibration point on the basic relationships of Eq. (7) where the H function is a constant, H_o, and comparing that with the usual expression for the C(T) geometry,

$$F_Y = BW(b/W)^\eta H_o = \Omega BW(b/W)\beta\sigma_Y \tag{15}$$

where Ω is a constraint parameter taking different values for plane strain and plane stress, σ_Y is a yield stress and β is a polynomial given by

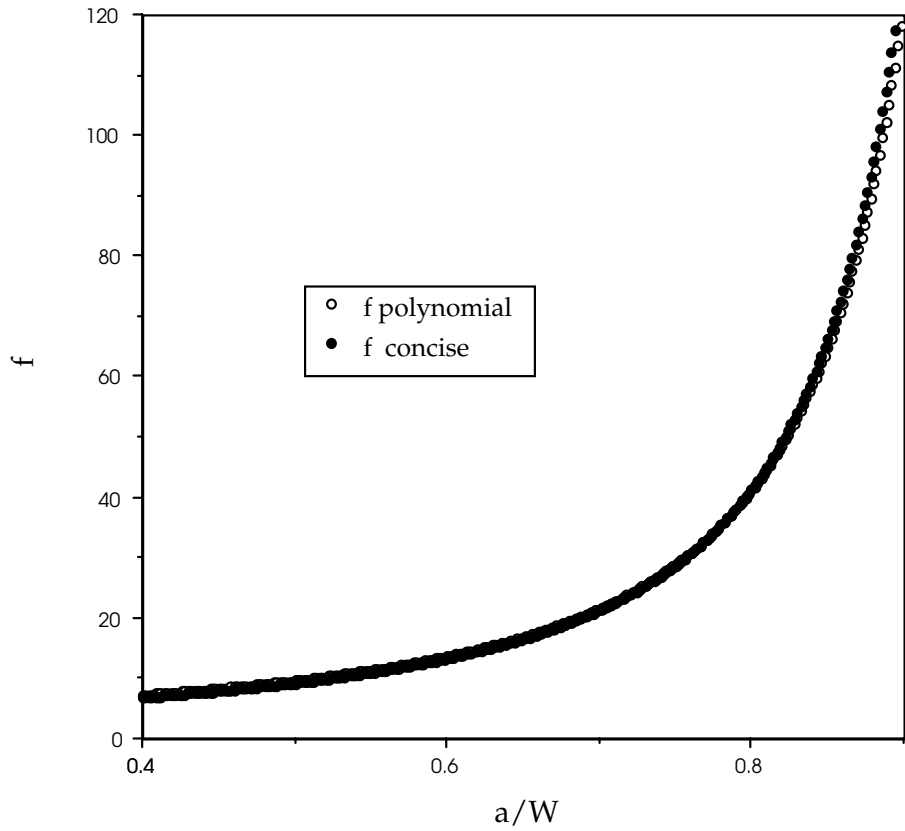$$\beta = \{4(a/b)^2 + 4(a/b) +2\}^{1/2} - \{2(a/b) + 1\} \tag{16}$$

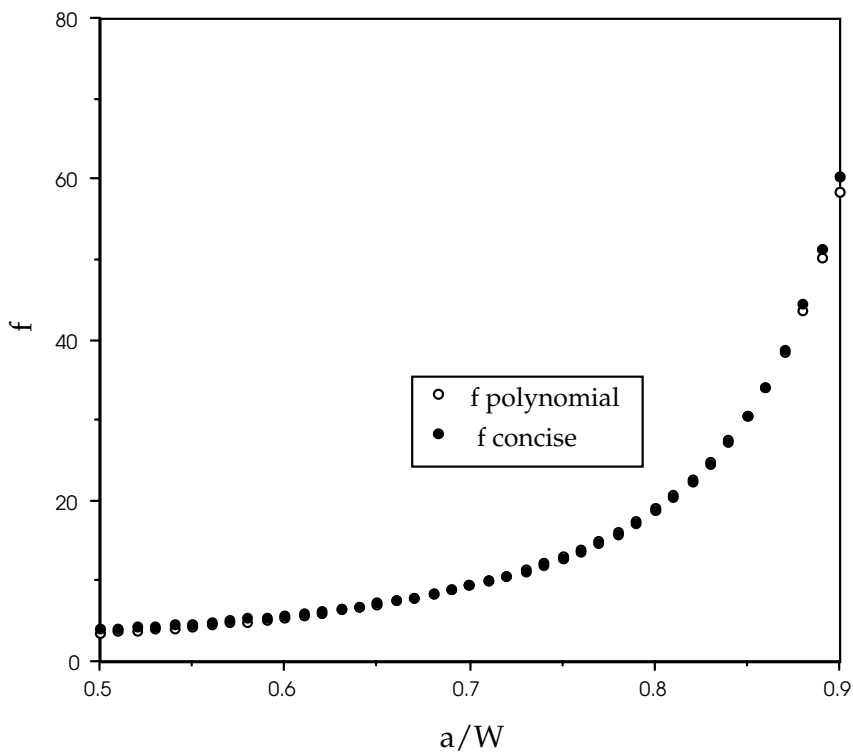*Figure 5:* f calibrations from polynomial and concise forms for C(T) geometry.

Figure 6: f calibrations from polynomial and concise forms for SE(T) geometry.

The polynomial form of the limit force and the concise form are compared in Figure 7 for the C(T) geometry where β(b/W) is plotted as a function of a/W in log-log format, and in Figure 8 for the SE(T) geometry where a similar factor is plotted versus a/W in log-log format. Almost all of the limit force expressions take on this simple form for two-dimensional cracks. The concise form for limit force then allows a simple relationship between K and limit force given by

$$K = \frac{F}{B\sqrt{W}}\left[\frac{\sqrt{\dfrac{\eta}{2\kappa}}}{\left(\dfrac{F_Y}{BWH_o}\right)^{\frac{\eta+1}{2\eta}}}\right] \qquad (17)$$

Here the bracket in Eq. (17) replaces the traditional polynomial form of the f(a/W) in the usual K expression. This way of relating K and F_Y may have some advantages in the formulation of calibration expressions.
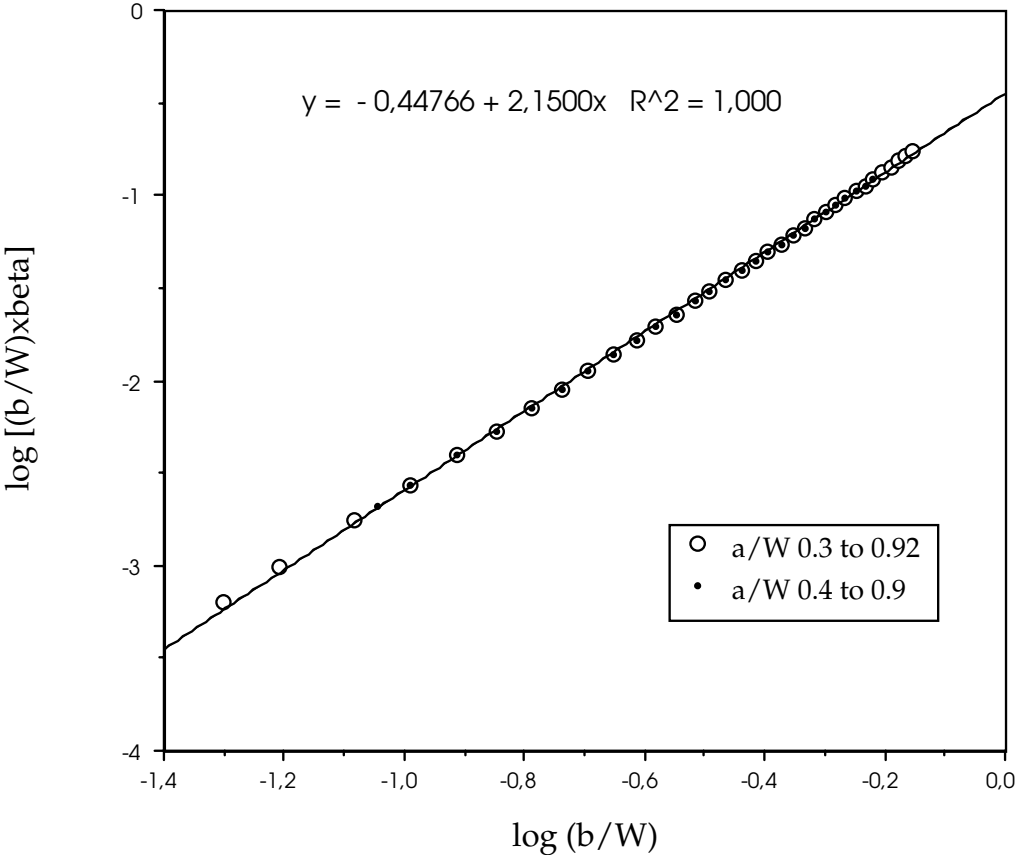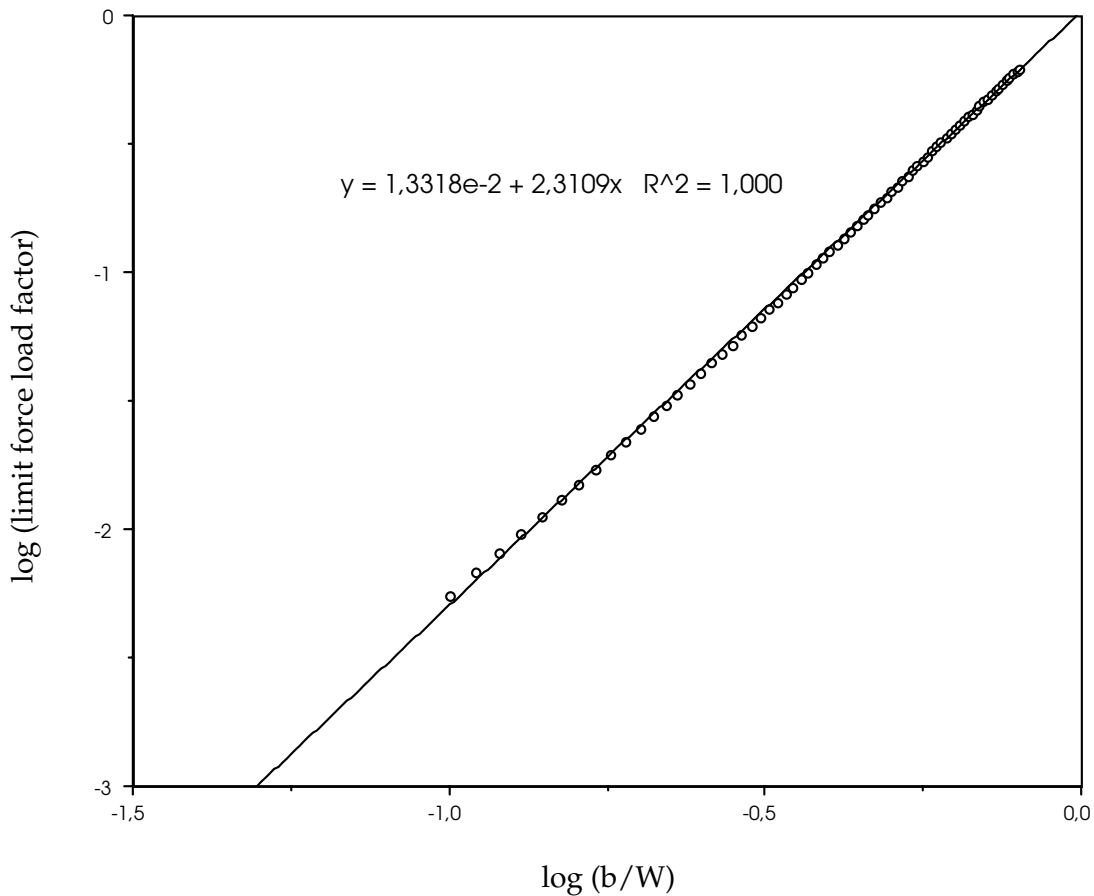

*Figure 7:* Log [beta(b/W)] vs log (b/W), C(T).

Figure 8: Log-log plot of limit force factor vs b/W for C(T) geometry.

7 CREEP DEFORMATION FORMULATIONS

The relationships among the fracture mechanics parameters can be used to formulate the creep deformation expressions that will be used in the correlation of creep cracking behavior and residual life prediction. The creep deformation parameters that will be studied are the traditional C^* and C_t parameters and the ETM ones based on the δ_5 parameter. The traditional parameters will be discussed first. These parameters will be formulated with the assumption that the separation relationship in Eq. (5) has a G function that is independent of the deformation process. That is, it is the same for creep deformation as it is for plastic deformation. This assumption has already been applied without verification to the formulation of the C^* and C_t parameters.

The creep deformation parameters used for fracture mechanics formulations must be discussed with a knowledge of the basic creep deformation processes. The basic material behavior under creep conditions is a deformation pattern that changes continuously as a function of time under constant force or stress conditions. This is

different from elastic and plasticity behavior in which deformation essentially remains unchanged under constant force conditions. The deformation change with time for creep behavior, creep strain rate, is one that begins more rapidly with the application of a force or stress and decreases until it reaches a constant value, Figure 9. At this point the creep deformation process is said to reach a steady-state creep condition. This steady state condition continues until geometry changes such as necking and internal damage cause a further increase in the creep deformation rate. The creep deformation process is then divided into three stages, Fig. 9, the initial more rapid but decreasing strain rate stage is called primary creep, the steady state creep stage is called secondary creep and the increasing strain rate stage tertiary creep. Since the tertiary creep stage is the beginning of a failure process, it is not considered in the evaluation of residual life. The primary and secondary stage creep regimes can be evaluated to define the parameters controlling creep cracking and residual life processes.
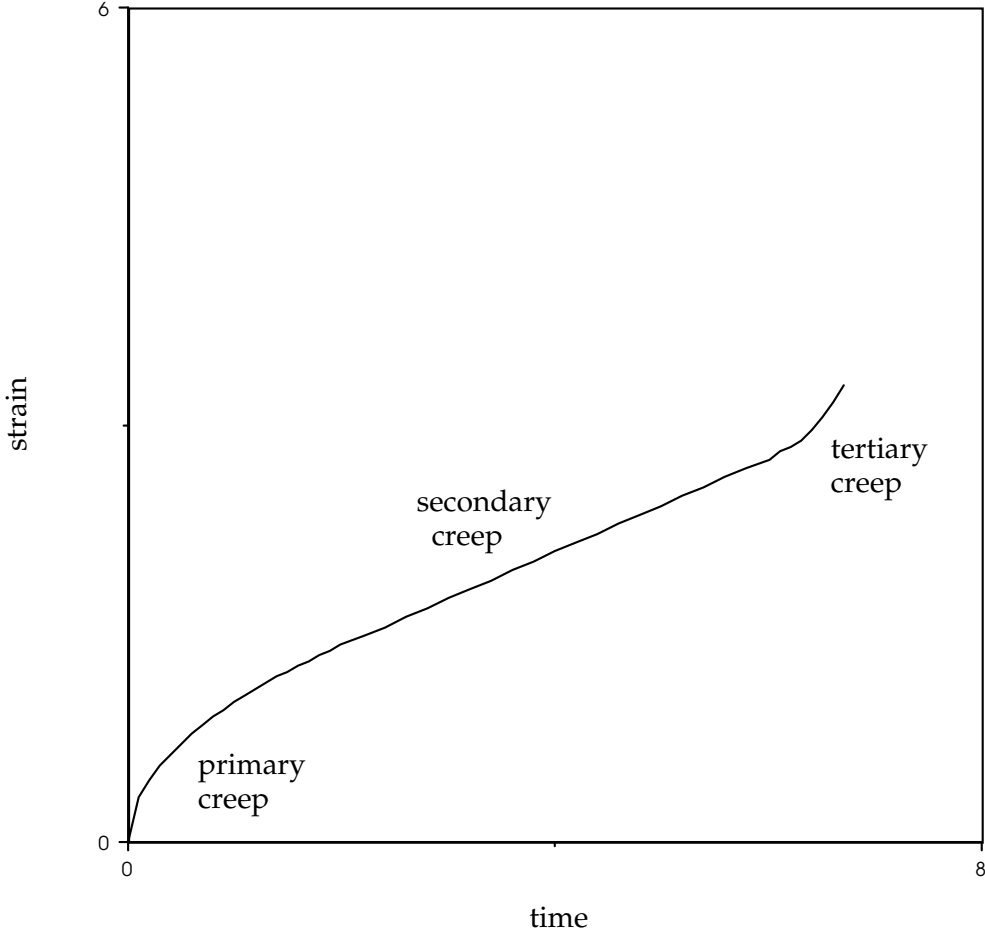
Figure 9: Schematic of creep strain versus time.

In the secondary stage of creep deformation the creep rate is not time dependent and is usually described as a function of stress with a power law (often known as Norton's law) given by

$$\dot{\varepsilon} = A\sigma^n \qquad (18)$$

where A and n are material parameters, A is a constant coefficient and n a constant exponent. The power law relating creep rate and stress has an analogy in the region of plasticity behavior in that a power law is often written to relate the plastic strain and the stress

$$\sigma = k(\varepsilon_{pl})^N \qquad (19)$$

where k and N are material parameters, k is a constant coefficient and N a constant exponent. By using this law in an analogy between plastic strain and creep strain rate and with n being analogous to $1/N$, many of the relationships that have already been developed for plasticity can be related to the steady state creep behavior with $\dot{\varepsilon}$ substituted for ε or displacement rate substituted for a displacement [18].

This analogy for developing creep deformation relationships from plastic deformation relationships depends on the separable nature of the functional forms as given in Eq. (5). The functional form of the C^* and C_t deformation parameters was first made assuming that all creep deformation was in the secondary creep stage and that the steady state power law relationship between creep stress and strain rate in Eq. (18) was valid. Later the primary creep stage was added to the formulation of the creep deformation parameters [18]. However, for this discussion the assumption of steady state creep and Eq. (18) will be made.

The creep deformation behavior that occurs in a specimen or structure containing a macroscopic crack is one that can be described in relation to a creep deformation zone that develops at the tip of the crack and the other dimensions of the body, namely the uncracked ligament. The creep deformation time periods have been divided into the three stages [18], small-scale creep (SSC), transition creep (TC), and extensive creep (EC). The process is described schematically in Figure 10, where the creep deformation categories are described for a constant applied force.

With the beginning of the loading elastic, plastic and creep deformation processes are likely to occur. With a constant applied force the elastic and plastic deformations are assumed to remain constant but the creep deformation is constantly changing with time. At the tip of the crack a growing zone of material undergoing creep deformation appears. As stated, the creep zone is assumed to be in a steady state creep regime. The creep zone that initially appears is one that is small compared to

the other dimensions of the specimen or structure, Fig. 10a. As time progresses, the creep zone grows to the state where it dominates the uncracked ligament of the body, Fig. 10c. This is referred to as extensive creep. In the time between small scale and extensive creep there is a period when the creep zone is large compared to the other dimensions and may dominate the elastic and plastic zones but cannot be said to dominate the entire uncracked ligament of the body. For this case the label transition creep is given, Fig. 10b. The determination of the appropriate regime is made with the creep characterizing parameters themselves. A transition time between SSC and EC is determined; this is labeled, t_T. Its form is given in the following section after the various creep parameters have been presented. The parameters that must be used to describe the creep cracking process depend on the stage of cracking behavior.
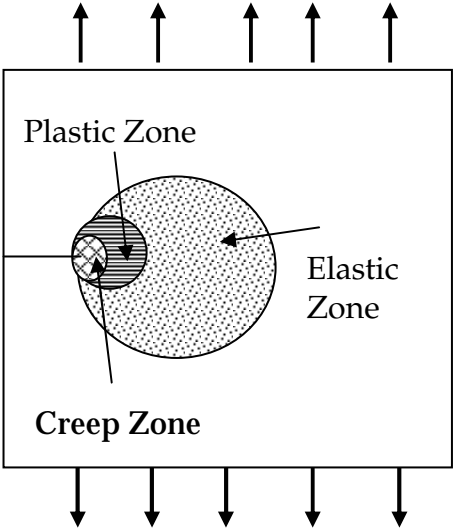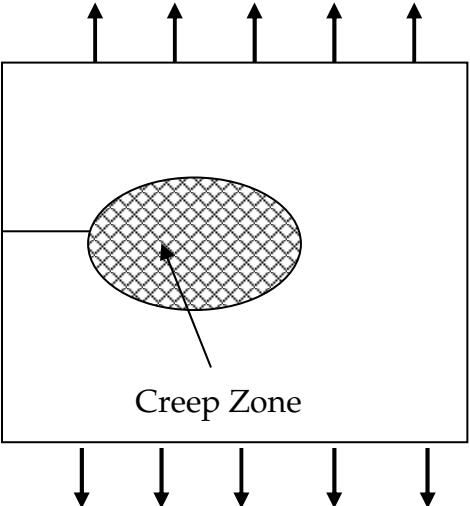

Figure 10a: Small Scale Creep, (SSC).
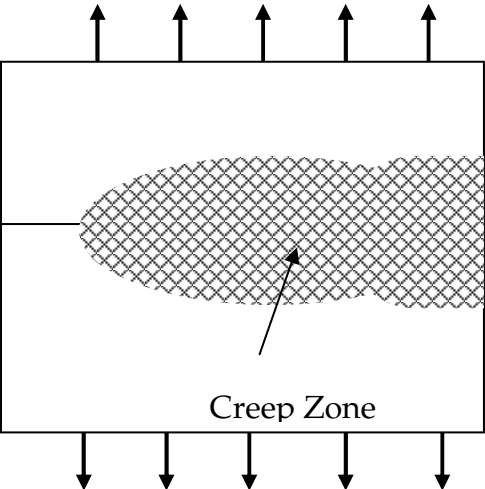

Figure 10b: Transition Creep, (TC).

Figure 10c: Extensive Creep, (EC).

Figure 10:
Three regimes of creep deformation in a structural element with a crack-like defect.

The traditional parameters used for creep cracking must take account of the region of creep behavior that the specimen or structure is presently undergoing, SSC, TC or EC. For extensive creep the parameter traditionally used for creep cracking is the C* parameter [2, 3]. It was originally given as a path independent line integral

$$C^* = \oint_{\Gamma} W^* dy - T_i \left(\frac{\partial \dot{u}_i}{\partial x} \right) ds \tag{20}$$

where W* is a strain energy rate density

$$W^* = \int_0^{\dot{\varepsilon}_{ij}} \sigma_{ij} d\dot{\varepsilon}_{ij} \tag{21}$$

and T_i is a traction vector along the integration path, Γ, u_i is a displacement vector and ds is an increment along the integration path. The C* path integral has an analogy to the J integral where all of the strains and displacements from J are replaced by their time derivative, indicated by the dot. Using this analogy C* can be given a energy time rate definition

$$C^* = -\frac{1}{B} \frac{dU^*}{da} \tag{22}$$

where dU* is the area between the force versus displacement rate plots for two identical bodies with differing crack length da and B is the thickness of the body.

Using this definition C* can be determined from data of force versus load-line displacement rate behavior in a specimen test by

$$C^* = \frac{\eta}{Bb} \int F d\dot{V}_C = \left(\frac{n}{n+1} \right) \frac{\eta F \dot{V}_C}{Bb} \tag{23}$$

where η is the same coefficient given for the J calibrations, and b is an uncracked ligament length in a test specimen, b = W – a, where W is a specimen width and $\dot{V}_C$ is the creep component of displacement. The integral represents the area under a plot of force, F, versus the creep component of the load-line displacement rate, $\dot{V}_C$, for a body undergoing creep deformation. C* is useful for correlating creep crack extension after reaching the extensive creep state that is defined for times, t >> t_T.

For times, t << t_T, defined as small scale creep, the parameter, C(t) was developed [19]. This is given by

$$C(t) = \frac{K^2}{E'(n+1)t}$$ (24)

where E′ is an effective elastic modulus, E for plane stress and $E/(1 - v^2)$ for plane strain. K is the crack-tip stress intensity factor. In the creep deformation equations it plays an important role in the formulation of parameters. The form of K used here is

$$K = \frac{Ff\left(\frac{a}{W}\right)}{B\sqrt{W}}$$ (25)

where f(a/W) is a geometry calibration factor which is available for many structural geometry forms. K solutions are given in many handbooks, sometimes in a different format [20]. The form of Eq. (25) should be used in formulating the creep parameters so a conversion should be made to that form if another is given.

To define the transition time, t_T, C* and C(t) are equated. Solving these gives a definition of the transition time, t_T as [19]

$$t_T = \frac{K^2}{E'(n+1)C*}$$ (26)

When the time is much larger than t_T, creep crack extension can be characterized by the C* parameter and when the time was much smaller than t_T, by C(t). For times around the transition time, these parameters are not valid. Saxena suggested the parameter C_t to go from small scale creep conditions to extensive creep [4]. It has the advantage that it spanned the entire region and is compatible with C* at times in the extensive creep range. C_t is given by

$$C_t = -\frac{1}{B}\frac{\partial U_t*}{\partial a}$$ (27)

where dU_t* is similar to the dU* area between two curves defined for C* in Eq. (22) but it is time dependent in the small scale creep regime. C_t then is a time dependent parameter. It can be defined from the K calibration for the small scale creep regime, SSC, where C_t is labeled (C_t)$_{SSC}$. For the entire regime from small scale creep to

extensive creep C_t is defined as

$$C_t = (C_t)_{SSC} + C*$$ (28)

For small scale creep under a constant force and for a stationary crack the $(C_t)_{SSC}$ parameter can be determined from force and displacement rate curve as

$$(C_t)_{SCC} = \frac{F\dot{V}_c}{BW}\frac{f'}{f}$$ (29)

where F and $\dot{V}_c$ are the force and creep component of displacement rate, f and f′ are the geometry factor from the K solution in Eq. (13) and its derivative with respect to a/W. $(C_t)_{SSC}$ can also be determined from K solutions so that it could be determined for many different geometries. This form is given by

$$(C_t)_{SSC} = \frac{2K^2}{E'W}\frac{f'}{f}\beta\dot{r}_c$$ (30)

where $\dot{r}_c$ is the rate of extension of the creep zone r_c, and β is a factor that determines how much of the creep zone is contributing to the $(C_t)_{SSC}$ parameter. Here β is usually taken as 1/3. The creep zone, r_c, is a function of time, t, is given by [18]

$$r_c = \frac{1}{2\pi}\alpha K^2 (EAt)^{\frac{2}{n-1}} F_{cr}$$ (31)

where A is the coefficient from the creep strain law in Eq. (18) and F_{cr} is a function that is taken to be 0.6 for plane stress and 0.3 for plane strain in most cases [16]. The term α combines several calibration factors

$$\alpha = \left(\frac{(n+1)^2}{2n\alpha_n^{n+1}}\right)^{\frac{2}{n-1}}$$ (32)

where n is the exponent from the Eq. (18) creep law and α_n^{n+1} is about 0.69.

Under a constant force and for a stationary crack, r_c can be differentiated and substituted into Eq. (30) to determine $(C_t)_{SSC}$. The result is

$$(C_t)_{SSC} = \frac{4K^4}{WE'(n-1)}\frac{f'}{f}\alpha\beta F_{cr}(EA)^{\frac{2}{n-1}} t^{\frac{3-n}{n-1}}$$ (33)

All of the terms in Eq. (33) have been defined previously. The exponent n is usually greater than 3 so the exponent of the time term, t, is negative and $(C_t)_{SSC}$ is steadily decreasing with time. As the time increases to values much greater than t_T, the $(C_t)_{SSC}$ term becomes small and C_t approaches C^*. Therefore, C_t is a parameter that covers all of the creep ranges and is compatible with C^* in the extensive creep range. For a more comprehensive description of the C based parameters refer to the book by Saxena [18].

8   ETM CREEP CRACKING PARAMETERS

The ETM based δ_5 parameters must be developed for the different creep time regions as was done for the C^* and C_t parameters. The ETM creep cracking parameters are based on the δ_5 parameter [5, 6]. The δ_5 parameter is a crack-tip opening displacement parameter measured over a gage length of 5 mm. It can be measured directly on a test specimen and can be related to other fracture parameters like K and J to use as a crack driving force parameter. The δ_5 parameter has the advantage that it can be easily measured on a specimen with a surface breaking defect and has no geometrical restrictions. For creep cracking under creep ductile conditions the δ_5 parameter, $\dot{\delta}_5$, has been suggested for use as a creep crack correlating parameter [21]. The parameter $\dot{\delta}_5$ has already been used as a creep crack extension correlating parameter [22]. It can be used for spanning the range from small-scale creep to extensive creep. In that way it is convenient for measurement of crack extension rates covering an extensive range of times. The application of the parameter, however, requires that it be calculated in different forms for each time range. In looking at ways to determine the $\dot{\delta}_5$ parameter for various structural type components, the analogies made for the C^* and C_t parameters will be used as models. Here again, the separability principle plays an important role.

The first step in developing the ETM creep parameters is to look at how they are used for the other deformation modes. For elastic and plastic deformation the ETM δ_5 model uses the following format for essentially elastic behavior. The parameter δ_5 is related to K for an essentially linear regime

$$\delta_5 = \frac{\beta_1}{E} K + \frac{K_{eff}^2}{mE\sigma_Y}\left(\frac{F}{F_Y}\right) \tag{34}$$

where, β_1 = 2.41 for plane stress and 2.09 for plane strain, m = 1 for plane stress and 2 for plane strain, F is the applied force, F_Y is a yield or limit force defined by a yield

stress σ_Y and K_{eff} is defined by

$$K_{eff} = \frac{F f\left(\dfrac{a_{eff}}{W}\right)}{B\sqrt{W}} \qquad (35)$$

and

$$a_{eff} = a + \frac{1}{2\pi}\left(\frac{K}{\sigma_Y}\right)^2 \qquad (36)$$

For fully plastic behavior the form used is

$$\frac{\delta_5}{\delta_{5Y}} = \left(\frac{F}{F_Y}\right)^{\frac{1}{N}} = \left(\frac{J}{J_Y}\right)^{\frac{1}{N+1}} \qquad (37)$$

where all of the parameters used in assessment, δ_5, force, F or J are divided by normalizing parameters δ_{5Y}, force, F_Y or J_Y which are calculated for $F = F_Y$.

For extensive creep the format used for plasticity can be extended into the creep regime by making use of the separability principle that allows the time rate parameter to be substituted for the strain or displacement parameter [16]. This gives a way to find $\dot{\delta}_5$ from force, F, or from C*:

$$\frac{\dot{\delta}_5 *}{\dot{\delta}_{5OC}} = \left(\frac{F}{F_{OC}}\right)^{n} = \left(\frac{C *}{C *_{OC}}\right)^{\frac{n}{n+1}} \qquad (38)$$

The parameter $\dot{\delta}_5 *$ is $\dot{\delta}_5$ for extensive creep. The parameters $\dot{\delta}_5 *$, F and C* are taken as ratios to calibration values of $\dot{\delta}_5, \dot{\delta}_{5OC}$, of force, F_{OC} and of C*, $C*_{OC}$. This calibration force, F_{OC}, has a similar function to that of the yield force in Eq. (37). It can be taken from calibrations given in the EFAM ETM 97 procedure for assessing the significance of crack-like defects in structures [23] with the stress σ_{OC} substituted for σ_Y. Therefore most of the calibrations needed for F_{OC} already exist. Similar to Eq. (37), Eq. (38) is a master curve that due to normalization describes the creep cracking parameter independently of geometry and size of the cracked component. It does, however, depend on the material through the creep exponent, n.

The inputs needed to determine the calibration values must be defined. The calibration stress σ_{OC} has to be taken as a point on the stress versus strain rate properties of the material given by Eq. (18), or as a point defined on a creep deformation curve. Since F_{OC} is an arbitrary calibration force, it can be arbitrarily chosen. However, it has to be a value that makes sense from a practical standpoint, that is the ratio F/F_{OC} should be about 1 in the extensive creep range. A suggestion of a value is the point where a strain of 0.002 is reached in transition time, t_T. Therefore, $\dot{\varepsilon}_{OC} = 0.002/t_T$ is a good first estimate to use with Eq. (18) to get σ_{OC}. Then σ_{OC} is given by

$$\sigma_{OC} = \left(\frac{\dot{\varepsilon}_{OC}}{A}\right)^{\frac{1}{n}} = \left(\frac{0.002}{t_T A}\right)^{\frac{1}{n}} \tag{39}$$

Choosing σ_{OC} by the transition time t_T makes it a function of both material and geometry and not material alone.

The calibration of $\dot{\delta}_{5OC}$ can be done experimentally from tests where δ_5 is measured as a function of force, displacement and time. It would be taken at the point of F_{OC} on a plot of δ_5 rate versus F. However, for an arbitrary component a value of $\dot{\delta}_{5OC}$ should be determined from other known parameters. A way to do this is with numerical calibrations for each structural geometry of interest. However, presently a set of numerical calibrations for $\dot{\delta}_{5OC}$ are not available. Therefore, if it could be done analytically from known calibration parameters, it would be an advantage. A way to do this analytically is being studied from the experimental results. Some suggestions are made later after the parameter relationships are defined.

For small-scale creep a definition of a parameter $\dot{\delta}_{5SSC}$ is needed. This can then be taken with $\dot{\delta}_5 *$ to get

$$\dot{\delta}_5 = \dot{\delta}_{5SSC} + \dot{\delta}_5 * \tag{40}$$

The form of $\dot{\delta}_{5SSC}$ can be taken from the format δ_5 of Eq. (34). Differentiating the small scale yield form of δ_5 given by Eq. (34), under constant force and for a stationary crack gives

$$\dot{\delta}_5 = \frac{2K_{eff}\dot{K}_{eff}}{mE\sigma_Y}\left(\frac{F}{F_Y}\right) \tag{41}$$

since the K and F terms are fixed, their derivatives are zero. $\dot{K}_{eff}$ can be taken from Eq. (35)

$$\dot{K}_{eff} = \frac{Ff'\left(\dfrac{a_{eff}}{W}\right)}{B\sqrt{W}}\frac{\dot{a}_{eff}}{W} \tag{42}$$

Defining a_{eff} in terms of a growing creep zone [18]

$$a_{eff} = a + \beta r_c \tag{43}$$

where all of the terms have been defined previously. Then, $\dot{a}_{eff}$ is

$$\dot{a}_{eff} = \beta \dot{r}_c \tag{44}$$

and

$$\dot{K}_{eff} = \frac{Ff'\left(\dfrac{a_{eff}}{W}\right)}{B\sqrt{W}}\frac{\beta \dot{r}_c}{W} \tag{45}$$

For small scale creep the value of K_{eff} is taken to be K and the values σ_{OC} and F_{OC} are substituted for σ_Y and F_Y. Then putting $\dot{K}_{eff}$ from Eq. (45) into Eq. (41) and substituting for $\dot{r}_c$ from the derivative of Eq. (31), a value of $\dot{\delta}_{5SSC}$ is given as

$$\dot{\delta}_{5SSC} = \frac{2K^4}{WmE\sigma_{OC}}\frac{f'}{f}\alpha\beta F_{cr}\left(\frac{F}{F_{OC}}\right)(EA)^{\frac{2}{n-1}}\left(\frac{2}{n-1}\right)(t)^{\frac{3-n}{n-1}} \tag{46}$$

Eq. (46) has a form similar to that in $(C_t)_{SSC}$ in Eq. (33). Comparing the two shows that $\dot{\delta}_{5SSC}$ is related to $(C_t)_{SSC}$ by

$$\dot{\delta}_{5SSC} = \frac{(C_t)_{SSC}}{m\sigma_{OC}}\left(\frac{F}{F_{OC}}\right) \tag{47}$$

This relationship is similar to that given between a crack tip opening displacement, CTOD and the J integral used for plasticity analysis. It suggests that there could be a

relationship between $\dot{\delta}_{5SSC}$ and $\dot{\delta}_{5OC}$. An approximation for $\dot{\delta}_{5OC}$ can be $\dot{\delta}_{5C}$ taken at time, t_T, however, calibrations should be done for many geometries to confirm this.

Alternate forms for $\dot{\delta}_5$ and $\dot{\delta}_{5C}$ could make it easier to calculate. An approximate form of the C_t parameter was suggested by Bassani et al. [24]:

$$C_t \approx \left[1 + \left(\frac{t_T}{t} \right)^{\frac{n-3}{n-1}} \right] C^* \tag{48}$$

This form could also be applied to $\dot{\delta}_5$.

$$\dot{\delta}_5 \approx \left[1 + \left(\frac{t_T}{t} \right)^{\frac{n-3}{n-1}} \right] \dot{\delta}_5^* \tag{49}$$

Using this form for large values of n, the expression becomes

$$\dot{\delta}_5 \approx \left[1 + \left(\frac{t_T}{t} \right) \right] \dot{\delta}_5^* \tag{50}$$

Substituting the value of t_T from Eq. (26) gives

$$\dot{\delta}_5 \approx \left[1 + \left(\frac{K^2}{E(n+1)C^*t} \right) \right] \dot{\delta}_5^* \tag{51}$$

and substituting from Eqs. (38) and (40)

$$\dot{\delta}_5 \approx \left[1 + \left(\frac{K^2}{E(n+1)C^*t} \right) \right] \frac{\dot{\delta}_{5OC}}{C_{OC}^*} C^* = \dot{\delta}_5^* + \dot{\delta}_{5SCC} \tag{52}$$

Therefore another form for $\dot{\delta}_{5SCC}$ might be

$$\dot{\delta}_{5SCC} \approx \left(\frac{K^2}{E(n+1)C^*t} \right) \frac{\dot{\delta}_{5OC}}{C_{OC}^*} C^* = \left(\frac{K^2}{E(n+1)t} \right) \left(\frac{\dot{\delta}_{5OC}}{C_{OC}^*} \right) \tag{53}$$

but since from Eq. (47)

$$\dot{\delta}_{5SSC} = \frac{(C_t)_{SSC}}{m\sigma_{OC}}\left(\frac{F}{F_{OC}}\right) \approx \frac{C^*}{m\sigma_{OC}}$$
(54)

at the calibration point, F_{OC},

$$\dot{\delta}_{5OC} \approx \left(\frac{K^2}{E(n+1)t_T m\sigma_{OC}}\right)$$
(55)

An estimate of C* can be taken from only the force, structural dimensions and creep law using the handbook analogy

$$C^* = Abh_1\left[\frac{P}{\Omega\gamma Bb}\right]^{n+1}$$
(56)

where A and n come from the creep deformation of Eq. (18) and Ω, γ and h_1 are given in Ref. [25].

An alternate form of $\dot{\delta}_5$ can be taken from the reference stress method of estimating C*. For a body with a defect the reference stress is based on a limit force solution, here used as F_{OC}. From [26], C* can be estimated from a reference stress, σ_{ref}, given by

$$\sigma_{ref} = \frac{F\sigma_Y}{F_Y}$$
(57)

The estimation for C* is given as [26]

$$C^* = \sigma_{ref}\dot{\varepsilon}_{ref}R'$$
(58)

where $\dot{\varepsilon}_{ref}$ is taken from the creep law in Eq. (18) corresponding to σ_{ref} and

$$R' = \left(\frac{K}{\sigma_{ref}}\right)^2$$
(59)

so

$$C^* = \frac{\dot{\varepsilon}_{ref}}{\sigma_{ref}} K^2 = A\sigma_{ref}^{n-1} K^2 \tag{60}$$

then $\dot{\delta}_5$ can be estimated as

$$\dot{\delta}_5 = \frac{C^*}{2m\sigma_{OC}} = \frac{A\sigma_{ref}^{n-1} K^2}{2m\sigma_{OC}} \tag{61}$$

Since $\dot{\delta}_5$ and C* are related at the calibration point, one parameter could be derived from the other. C* is calculated but δ_5 is measured; however, most of the creep crack growth rate date are developed in terms of C*. It would be easy to develop C* from the δ_5 measurement, since that is a direct measurement. A direct relationship between δ_5 rate and C* comes from Eq. (25)

$$\left(C^*\right)_{OC} = \sigma_{OC}\left(\dot{\delta}_5\right)_{OC} \tag{62}$$

This allows a direct calculation of the C* calibration when δ_5 has been measured; however, it requires a value of the calibration stress, σ_{OC}. The definition in Eq. (39) is one choice but t_T must first be calculated from other parameters that are also calculated. One way to solve this is to use a direct estimate of σ_{OC} from

$$\dot{\varepsilon} = \frac{\dot{\delta}_5}{1mm} \tag{63}$$

at the calibration point. Then, using Eq. (62), the value of the calibration $(C^*)_{OC}$ is

$$\left(C^*\right)_{OC} = \frac{\left[\left(\dot{\delta}_5\right)_{OC}\right]^{\frac{n+1}{n}}}{\left(A \bullet 1mm\right)^{\frac{1}{n}}} \tag{64}$$

Since the calibration point is arbitrary, Eq. (64) could work across a range of $\dot{\delta}_5$ values so that in general it becomes

$$C^* = \frac{\left(\dot{\delta}_5\right)}{\left(A \bullet 1mm\right)^{\frac{1}{n}}} \tag{65}$$

This allows C* to be calculated directly from $\dot{\delta}_5$.

In the following sections, some of these forms are evaluated experimentally to try to decide which forms give the best estimation of measured values.

9 EXPERIMENTAL DETAILS

The material used in this study is a Mg AZ31 alloy. It has chemistry and room temperature mechanical properties as given in Table 1. It was supplied as a 6 mm thick plate in the annealed condition. To develop the creep deformation properties tensile specimens with cross section of 8 mm wide by 6 mm thick were tested, two at room temperature and nine at 150 °C. To develop the creep deformation properties for cracked bodies, compact specimens with blunt notches of different notch lengths were tested. Also, some identical specimens with fatigue precracks were tested. The compact specimens had dimensions of thickness, B equal to 6 mm, and of width, W, equal to 50 mm. The notched specimens had notch lengths of 20, 25, 30, 35 and 40 mm. This corresponds to a/W ratios of 0.4, 0.5, 0.6, 0.7, and 0.8. The precracked specimens had crack lengths corresponding to a/W of about 0.5. Sketches of the tensile and compact specimen geometries are given in Figures 11a and 11b. All specimens were machined such that the loading was applied in the rolling direction of the plate.

Table 1: Chemical and mechanical properties of the Mg AZ31 alloy:

Chemical composition of AZ31;

Al	Zn	Si	Mn	Cu	Ni	Fe	Mg
3.07	1.07	< 0.005	0.008	0.002	0.004	0.003	balance

Room temperature mechanical properties (rolling direction).

Yield Strength [MPa]	Ultimate Tensile Strength [MPa]	Reduction in Area [%]
95.4	233.1	18.4

Tensile specimens tests were conducted using two strain rates at room temperature, 2×10^{-6}/s and 6×10^{-5}/s, five different strain rates between 1×10^{-7}/s and 8×10^{-6}/s at 150 °C, and at four different constant force levels, corresponding to stress levels between 50 and 90 MPa. For the notched compact specimens five different notch depths were tested at 150 °C under constant displacement rates, 5 and 10 μm per hour. Several precracked specimens were tested, one at room temperature and four at 150 °C. The precracked specimens were tested at displacement rates between 0.5 and 50 μm/hr. Except for the specimen tested at 0.5 μm/hr, they exhibited both crack initiation and crack extension. Initiation was detected by an electrical potential

drop system. The deformation evaluations for these specimens were taken before crack initiation so that a constant crack length was maintained. The tests were conducted in a computer controlled screw driven test machine that is able to apply a constant load or constant displacement rate. Typical test times were in the order of several weeks to several months.
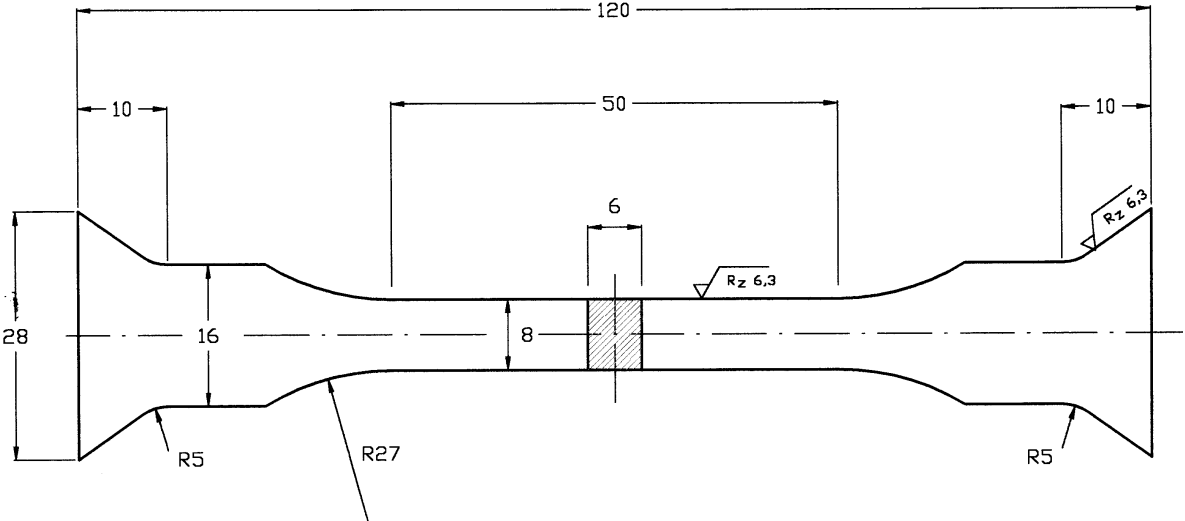

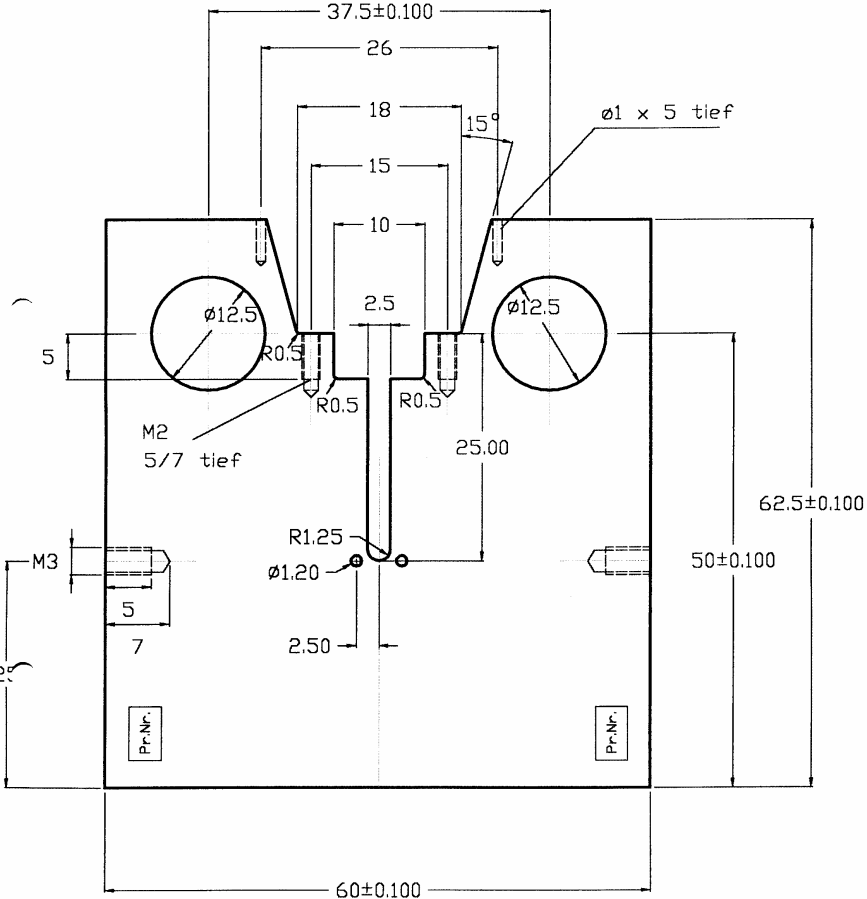*Figure 11a:* Tensile specimen (dimensions in millimeter).

Figure 11b:
Compact specimen with blunt notch (dimensions in millimeter).

10 TENSILE TESTS RESULTS

The room temperature stress versus strain curves were conducted at two strain rates about 3×10^{-3} and 1.3×10^{-4} per second. The stress-strain curves are presented in Fig. 12. The two rates gave almost identical results suggesting that there is little creep deformation for the material at room temperature.
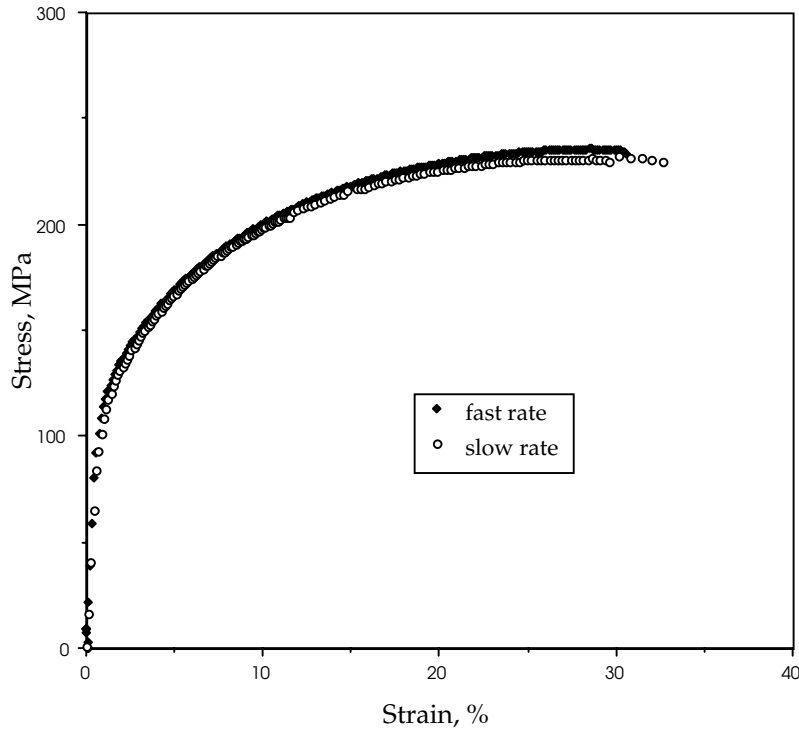
Figure 12:
Room temperature stress-strain results for Mg alloy.

At 150 °C a typical stress versus time curve at constant strain rate is shown in Figure 13a and a typical strain versus time curve at constant stress is shown in Fig. 13b. The constant strain rate tests show increasing stress until a steady state condition is reached where the stress reaches a relatively constant value. The stress in Fig. 13a shows some variation due to temperature fluctuation during the test. The constant stress test showed a typical pattern of three stage creep strain behavior, Fig. 13b, first an initial region with a fast but decreasing strain rate, second a steady state region with a constant strain rate and third a region of increasing strain rate.

The tensile test results are summarized in Figure 14. in terms of strain rate versus stress. Strain rate is measured for steady state conditions. The two methods of loading gave similar results; however, the constant strain rates results were a little lower than the constant stress results. On a log-log plot, Fig. 14, they give a reasonably straight line so that a power law like that of Eq. (18) was fit to the results for the all values as well as the constant strain rate and constant stress values. The combined results gave a power law fit for the combined results that was

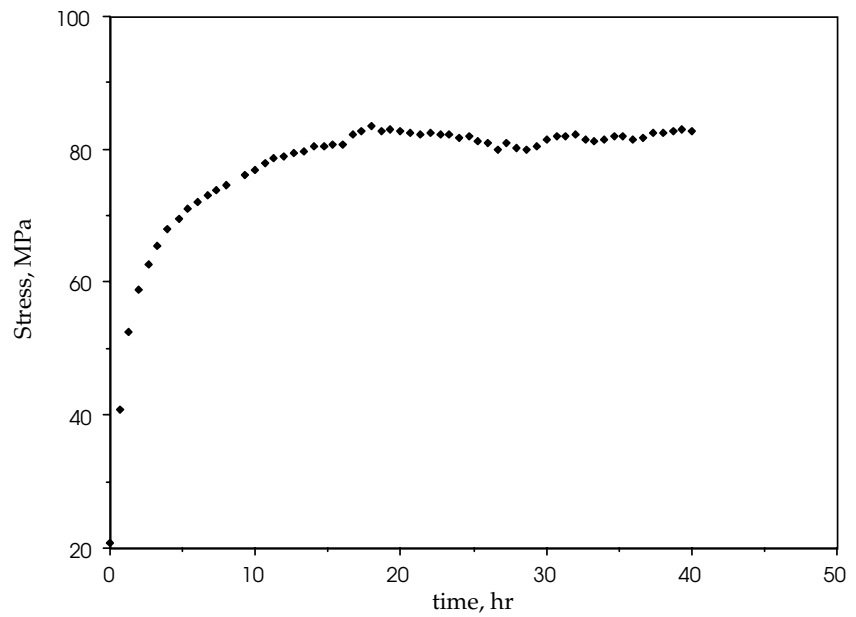$$\dot{\varepsilon} = 3.89 x 10^{-22} \sigma^{9.84} \tag{66}$$

For the constant stress tests alone the fit gave
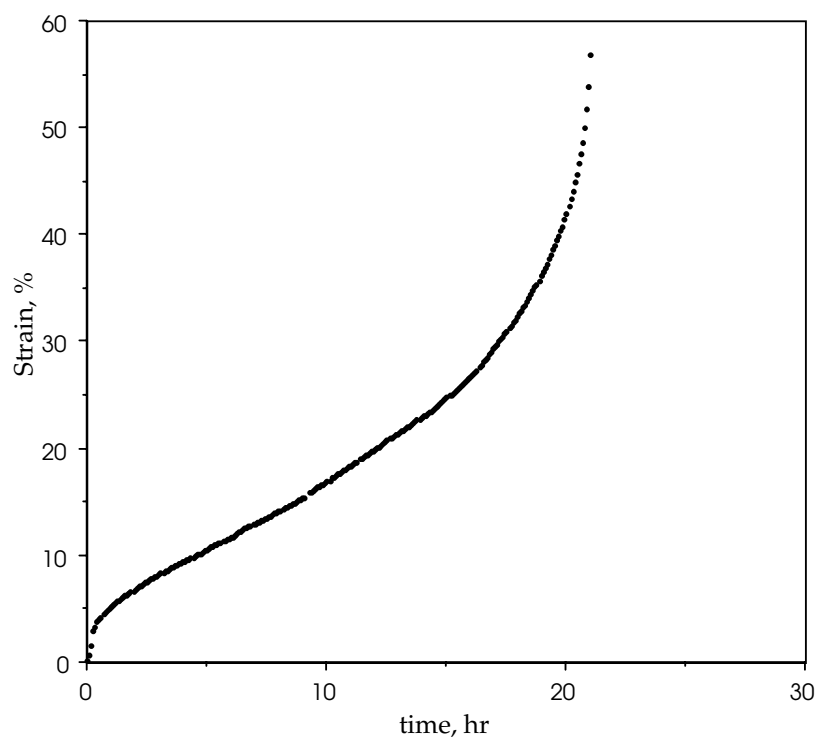
$$\dot{\varepsilon} = 2.29x10^{-20}\sigma^{8.9} \tag{67}$$

and for the constant strain rate tests alone the fit gave

$$\dot{\varepsilon} = 1.138x10^{-25}\sigma^{11.7} \tag{68}$$

Figure 13a:
Stress versus time
for a tensile test under
constant strain rate of
0.0037/hr.

Figure 13b:
Strain versus time for a
tensile specimen under a
constant stress of 90 Mpa.

Although the exponents are different, over the range of the main data there is not so much difference in the predicted rates given by the fits. The fitted lines are also included in Figure 14. It can be seen there that all of the fitted lines are similar and that the difference in slopes are influenced by single points that lie at the high or low end of the data spread. For the purpose of developing the creep deformation parameters, the fit to the combined data is used, the one given by Eq. (66).
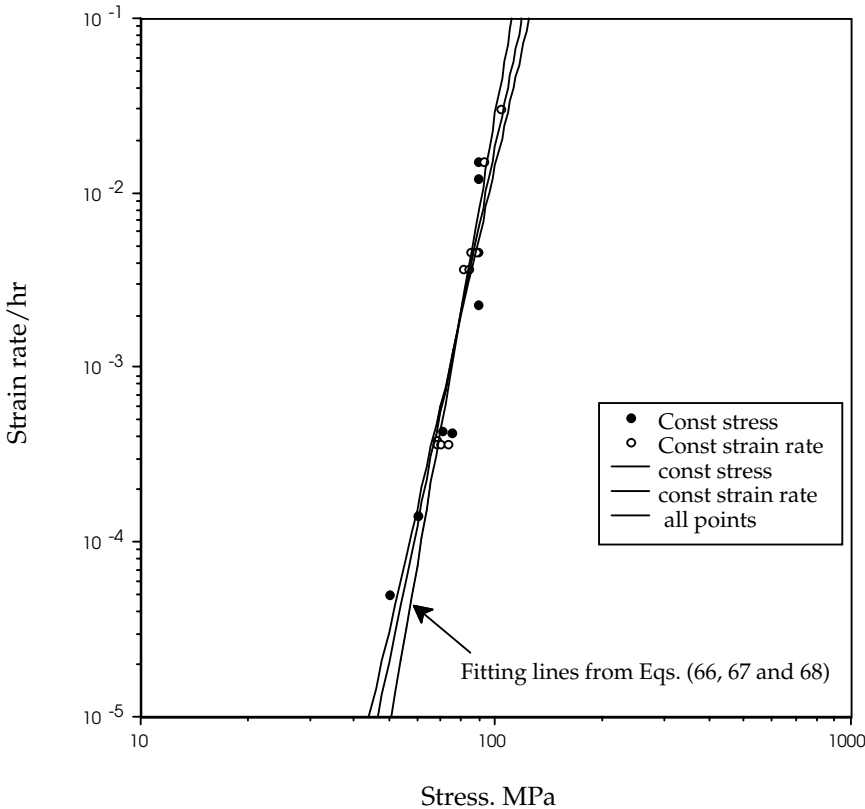
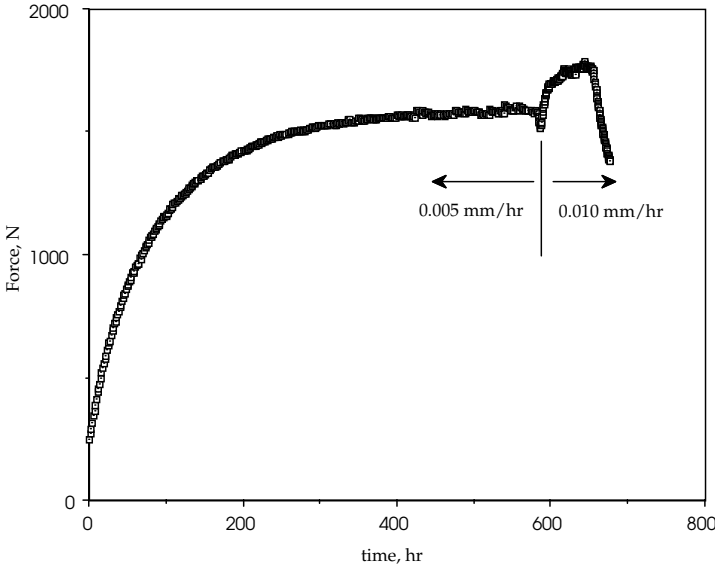*Figure 14:*
Strain rate versus stress with power law fits.

11 NOTCHED COMPACT SPECIMEN TEST RESULTS

The initial tests on the blunt notched compact specimens were with constant load-line displacement rates. Nominally, two load-line displacement rates were used,5 μm per hour and 10 μm per hour. Although five notch lengths were used, the notch corresponding to a/W of 0.4 did not give good results because the short notch length caused the forces to be too large and the loading pinholes were stretched. Only the data during the early part of the test were used. Also the specimen with notch length of 35 mm saw only one displacement rate.

The load versus time for the specimen with notch of 25 mm, a/W = 0.5, is shown in Figure 15. The load increases under a constant displacement rate and reaches a steady-state value. When the displacement rate is increased from 5 to 10 mm per hour, a new steady-state force is reached but in a much shorter time. In all tests of

the compact specimens the force, load-line displacement and δ_5 are measured. The load-line displacement and δ_5 are plotted versus time in Figure 16 for the same specimen, a/W = 0.5. The result shows that the load-line displacement has a constant rate. However, δ_5 increases at a slower, non-steady rate and reaches a steady state rate by the time the load has reached a steady state condition. This can be seen as well in Figure 17 where only δ_5 is plotted as a function of load-line displacement. In the evaluation of the rates only the steady state region was considered. Since there is sometimes a little scatter in some of the results, a fit was made to the displacement versus time curves in the steady state region to establish a rate.

Figure 15:
Force versus time for
compact specimen with a/W = 0.5.

Figure 16:
Load-line displacement
and delta-5 versus time
with a/W = 0.5.
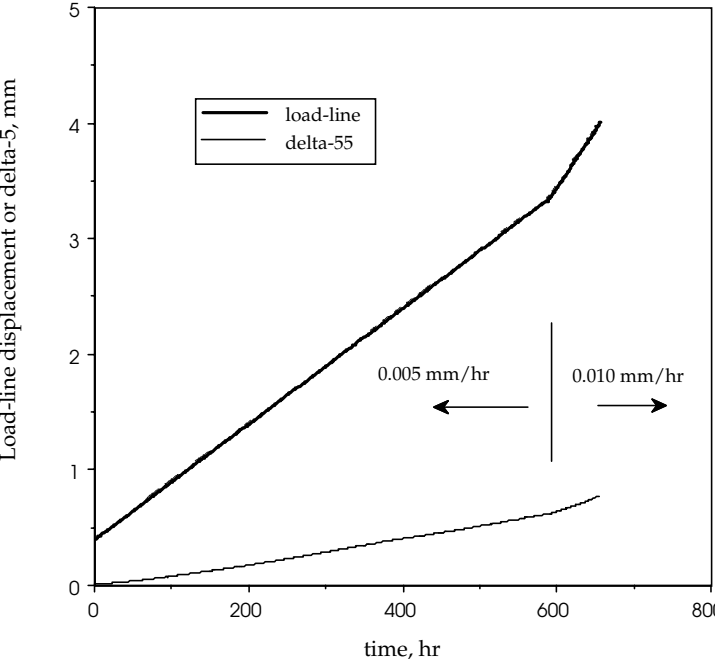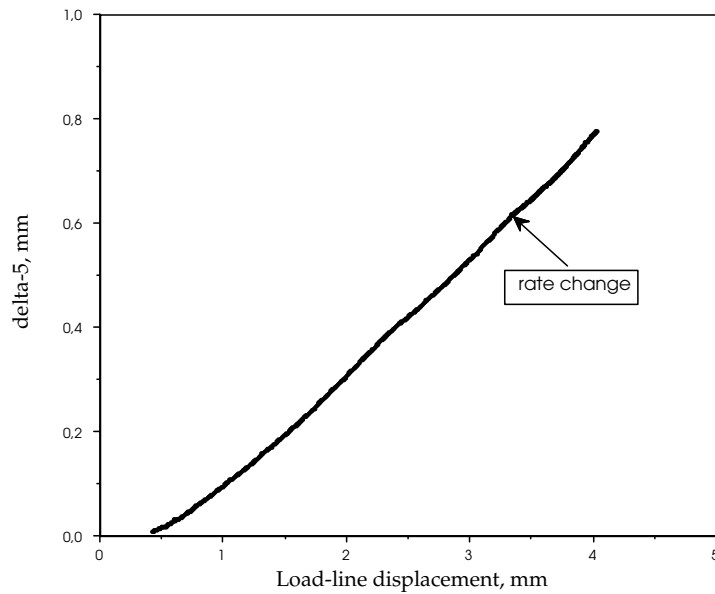
Figure 17:
Delta-5 versus load line displacement for a constant displacement rate with a step change, a/W = 0.5.

12 SEPARATION EVALUATION

Separation can be evaluated by plotting the ratio of the forces at the different displacement rates. The ratio was made taking the forces at a/W = 0.6 for the denominator. The results of the force versus displacement rate data are shown in Figure 18. The force ratio results are shown in Figure 19. These are done to evaluate the separability requirement that is normally written as a load ratio requirement.

$$\frac{F(a_i)}{F(a_j)} = Const \tag{69}$$

and is not a function of $\dot{V}_c$.

The separation load ratios should show a nearly constant ratio for the two displacement rates for a given a/W. This appears to be very nearly so in Figure 19. If the load separation does not hold for the creep results, then the use of the plasticity equations for the creep is not completely justified. However, it appears that the separation criterion is satisfied and the use of the plasticity equation formats justified. The load ratio result can also help to define the G(b/W) function that is the crack length dependence of the force and equation. For plasticity G(b/W) has the form

$$G(b/W) = BW(b/W)^\eta \tag{70}$$

where η takes a constant value of about 2.2 for plastic deformation. This form can be evaluated from the load ratio results. The results from Fig. 19 show a similar form

with an η value of about 2.3. This is of the correct order, for the elastic deformation of the C(T) specimen η = 2.28. This result appears to confirm the requirement of the similarity of the G function between plastic deformation and creep deformation rate. To further evaluate both the separation requirement and the form of the equations a finite element modeling of the creep behavior will be conducted.

Figure 18:
Force versus displacement rate for the notched compact specimens.
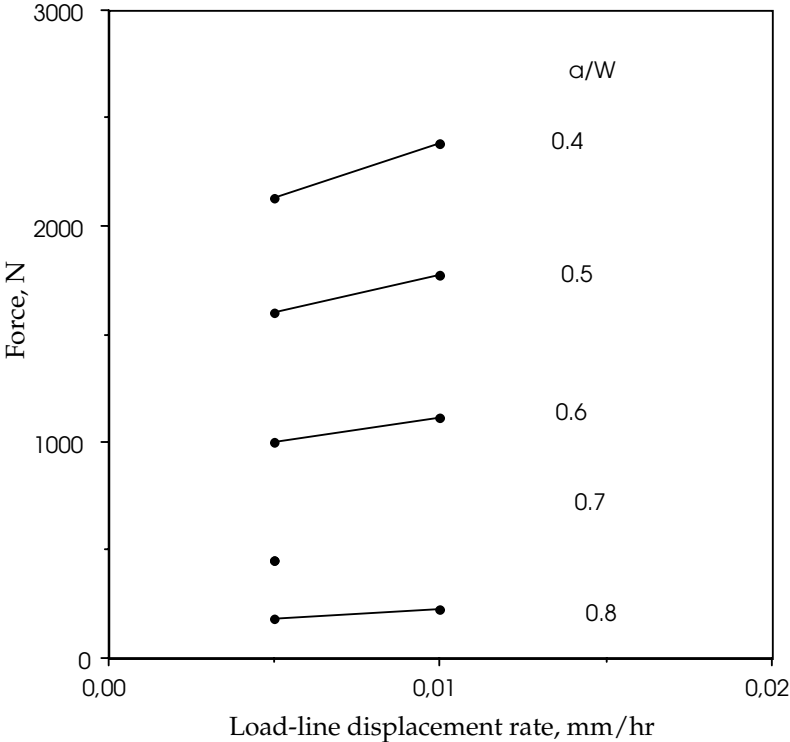
Figure 19:
Force ratios versus displacement rate.
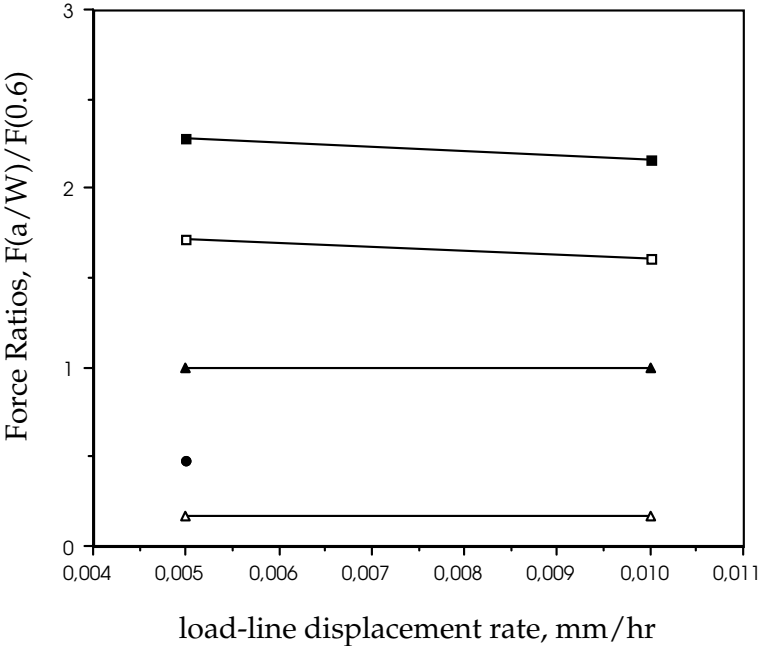
13   EVALUATION OF THE PARAMETERS

The C based and δ_5 based parameter expressions in the above section can be evaluated from the data that is available. A summary of all values obtained for the parameters evaluated is given in Table 2. The evaluation was made only under steady-state conditions. The establishment of a steady-state regime was based on the time t_T given by Eq. (26) and the appearance of reaching a constant load in the displacement rate controlled loading. The t_T time depended on the conditions of the test and the crack length. In general it ranged from about 30 hours to less than one hour. The time necessary to reach a steady load was always much more than this value of t_T. Figure 15 shows that for this case, blunt notched specimen with a/W = 0.5, it was several hundred hours.

The evaluation of the calibration forms included $\dot{\delta}_{5OC}$ form in Eq. (55), and the $\dot{\delta}_5$ estimation forms of Eqs. (46) and (61). The form in Eq. (46) is time dependent so it was taken at t_T. The form in Eq. (61) is time independent. The results for all of the $\dot{\delta}_5$ evaluations are shown in Figure 20 where $\dot{\delta}_5$ is plotted versus the specimen identification. The results are also given in Table 2a. The evaluations were made for two blunt notched specimens, TC-05 and TC-06 and for two precracked specimens, TC-09 and TC-13. The deformation in the precracked specimen was evaluated at a steady state condition before any crack extension began. This was monitored with an electrical potential drop system. All of the specimens except for TC-13 have an a/W value of about 0.5, TC-13 has a/W of 0.7.

The $\dot{\delta}_5$ results for all of the a/W = 0.5 show a consistent trend. The form given in Eq. (55) gives the lowest value. The forms of $\dot{\delta}_5$ given in Eqs.(46) and (61) are higher than the measured value for the a/W of 0.5 specimens. The results are plotted on a log scale because they can differ by an order of magnitude from one specimen to another. Therefore, differences in results may be difficult to evaluate. The result from Eq. (55), however, is closest to the measured values. For the deep notch specimen, TC-13 the measured value is larger than any of the results given by the equations but the estimated values take the same order as with the a/W of 0.5 results. In all of the estimations, the order of magnitude is correct between estimation and measured values, that is, they agree within a factor of 2 to 5. With more test results fitting constants could be introduced to allow the estimation formulas to be adjusted to better predict the measured values.

For the steady-state extensive creep conditions, the $\dot{\delta}_5$ of Eq. (38) can be evaluated in the tests that had two displacement rates. These are given in Table 2c and Figure 21. To evaluate the ratio in Eq. (38), the measured value $\dot{\delta}_5$ at the first displacement rate was used as the value $\dot{\delta}_{5OC}$ and the first force as F_{OC}. The value of $\dot{\delta}_5$ can then be evaluated from any applied force, F. The ability of Eq. (38) to predict the $\dot{\delta}_5$ at one

force from the $\dot{\delta_5}$ at another force is a way of confirming that the exponent, n, of Eq. (18) for the tensile creep results is the correct one for the specimen creep deformation as characterized by $\dot{\delta_5}$, that is, Eq. (38) is correct.

Table 2: Evaluation of the creep parameter forms.

Table 2a: Specimens used and input parameters;

Specimen No.	Condition	a/W	Initial $\dot{V_c}$, mm/hr	Force, N	K, MPa√m
TC-09	notched	0.50	0.005	1600	11.52
TC-13	notched	0.70	0.005	1930	14.77
TC-06	precracked	0.512	0.05	450	8.87
TC-05	precracked	0.510	0.0005	1194	7.23

*Table 2b:* Evaluation of $\dot{\delta_5}$ estimation forms;

Specimen No.	$\dot{V_c}$,mm/hr	$\dot{\delta_5}$, measured mm/hr	$\dot{\delta_5}$, Eq. (55) mm/hr	$\dot{\delta_5}$, Eq. (61) mm/hr	$\dot{\delta_5}$, Eq. (46) mm/hr
TC-09	0.005	1.12e-3	1.7e-3	2.39e-3	3.68e-3
TC-06	0.05	1.78e-2	1.88e-2	2.71e-2	4.28e-2
TC-05	0.0005	1.4e-4	1.42e-4	1.98e-4	3.24e-4
TC-13	0.005	6.0e-4	2.64e-4	2.95e-4	4.4e-4

*Table 2c:* Evaluation of $\dot{\delta_5}$ from Eq. (38);

Specimen No.	a/W	Force 1, N	Force 2, N	$\dot{\delta_5}$ 1, meas. mm/hr	$\dot{\delta_5}$ 2, meas. mm/hr	$\dot{\delta_5}$ 2, estimate mm/hr
TC-7	0.4	2130	2380	9.4e-4	2.5e-3	2.8e-3
TC-09	0.5	1600	1770	1.12e-3	2.45e-3	3.1e-3
TC-11	0.6	1000	1110	6.8e-3	1.87e-3	1.9e-3

Table 2d: Evaluation of C* formulas.

| Specimen No.	$\dot{V_c}$,mm/hr	C*, Eq. (23), MPa-m/hr	C*, Eq. (56), MPa-m/hr	C*, Eq. (60), MPa-m/hr	C*, Eq. (65), MPa-m/hr
TC-09	0.005	1.09e-4	1.19e-4	3.36e-4	8.5e-5
TC-06	0.005	1.16e-3	1.62e-3	4.73e-3	1.78e-3
TC-05	0.05	7.45e-6	8.0e-6	1.48e-5	7.45e-6
TC-013	0.0005	4.9e-5	1.67e-5	3.74e-5	4.4e-5
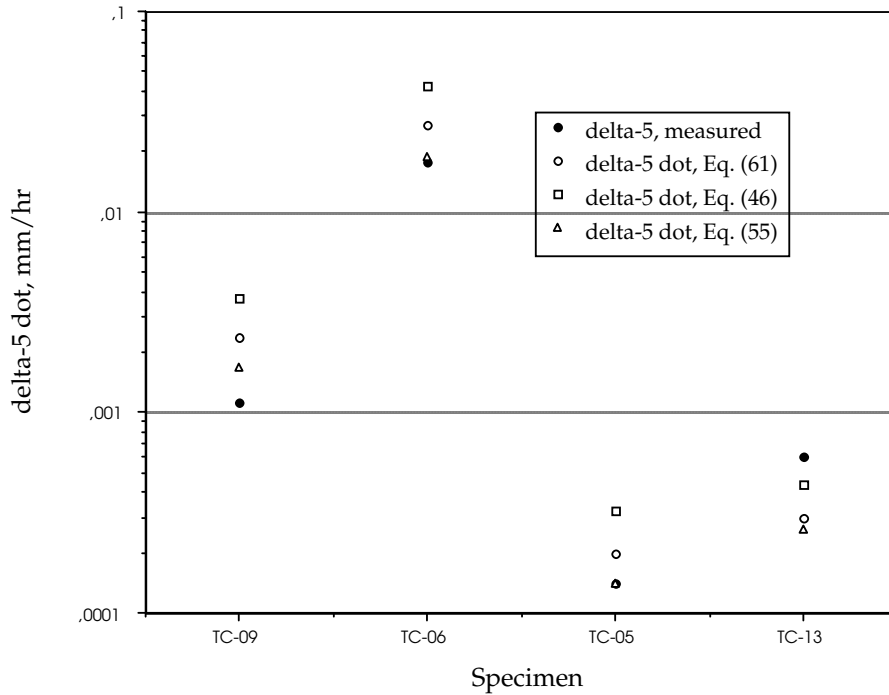
Figure 20:
Experimental
evaluation of delta-5
dot forms.
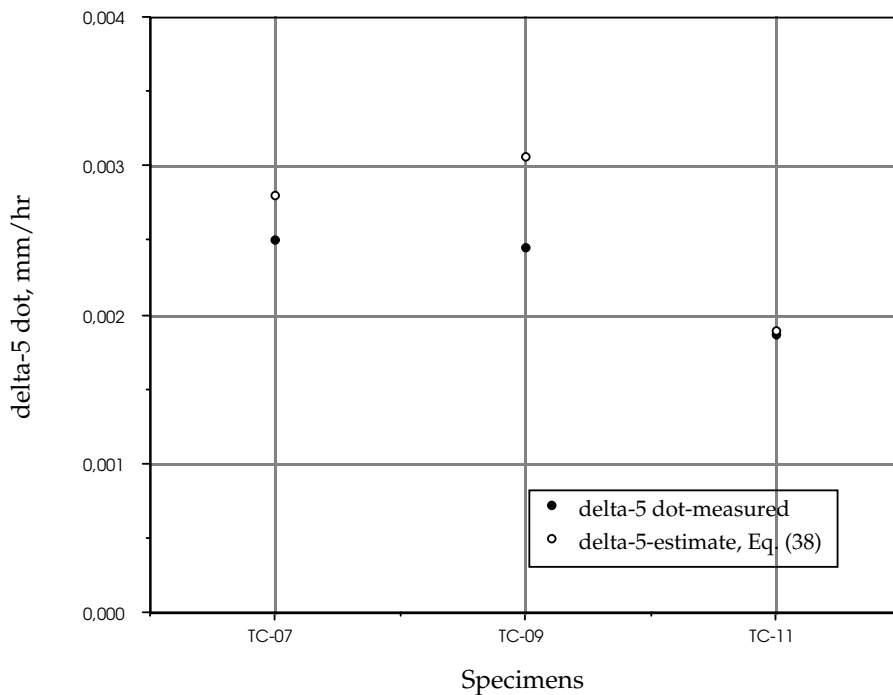
Figure 21:
Evaluation of **delta-5
dot** from Eq. (38).

The results in Fig. 21 are plotted on a linear scale so that the agreement is fairly good. A way to look at the creep deformation laws can also be taken from the fit to a log-log plot of force versus load line deformation rate. This was done for the specimens with a nominal a/W value of 0.5. The result given in Figure 22a showed that the exponent between steady state force and the creep deformation rate was about 9.0, in the range of values given by the tensile fits of Eqs. (66) to (68). A similar plot of $\dot{\delta}_5$ versus load gave the same slope of slope of 9.0, Figure 22b.

Figure 22a: Load-line displacement versus force with fit for a/W = 0.5.
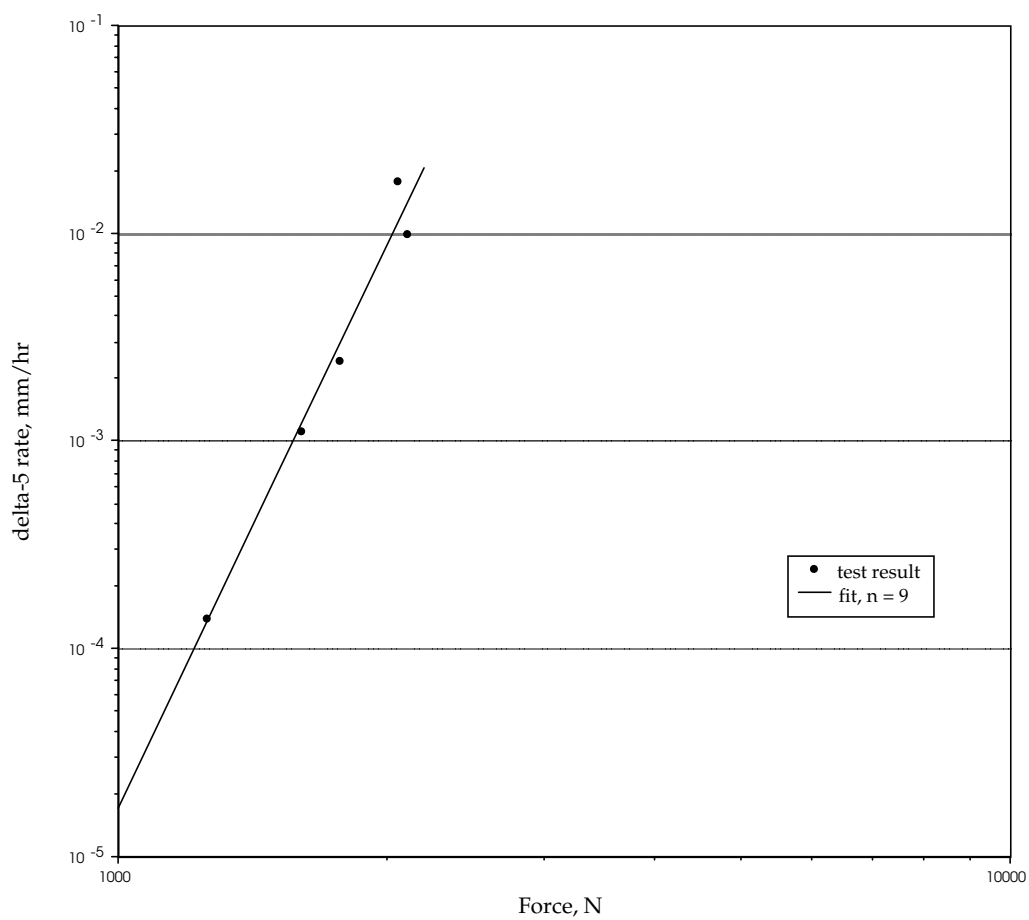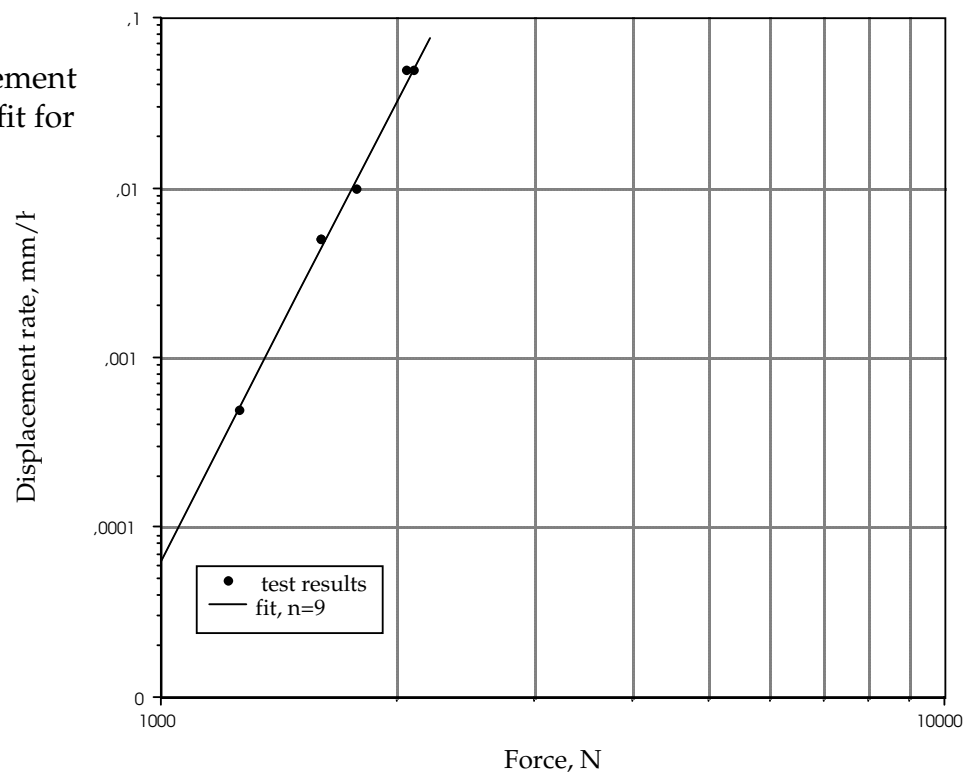
Figure 22b: Delta-5 rate versus force with fit for a/W = 0.5.

A calibration of the C* parameters can be made for the formats given in Eqs. (56), (60) and (65). Eq. (56) is the handbook analogy, Eq. (60) an estimation form of C* and Eq. (65) is the direct estimate of C* from $\dot{\delta}_5$. The exact value for C* is taken from Eq. (23) which uses the experimental results to determine C*. The results are given in Table 2d and in Figure 23. The same group of specimens used for the $\dot{\delta}_5$ evaluations was used here. The plot is also with a log scale. The results show a consistent ordering as was observed for the $\dot{\delta}_5$ evaluations. The direct estimate from $\dot{\delta}_5$, Eq. (65), gives the best result. The Handbook estimation formula of Eq. (56) is also close to the experimental result and the estimation of Eq. (60) shows a greater difference. The estimations are all larger than the experimental value when a/W is nominally 0.5 but lower than the measured value when a/W is 0.7.
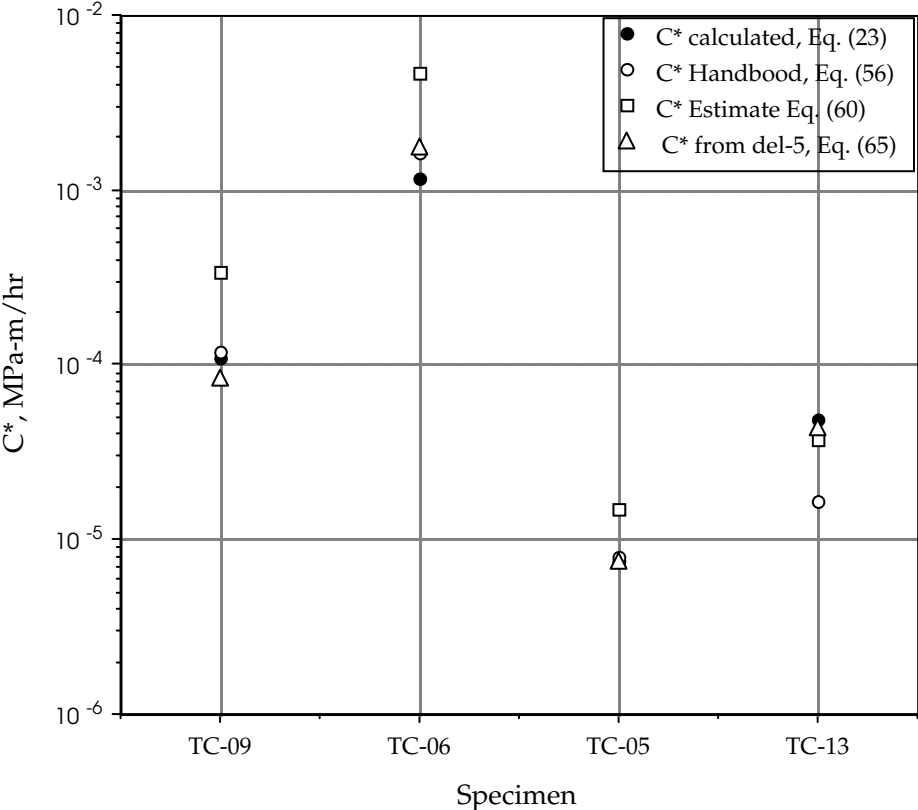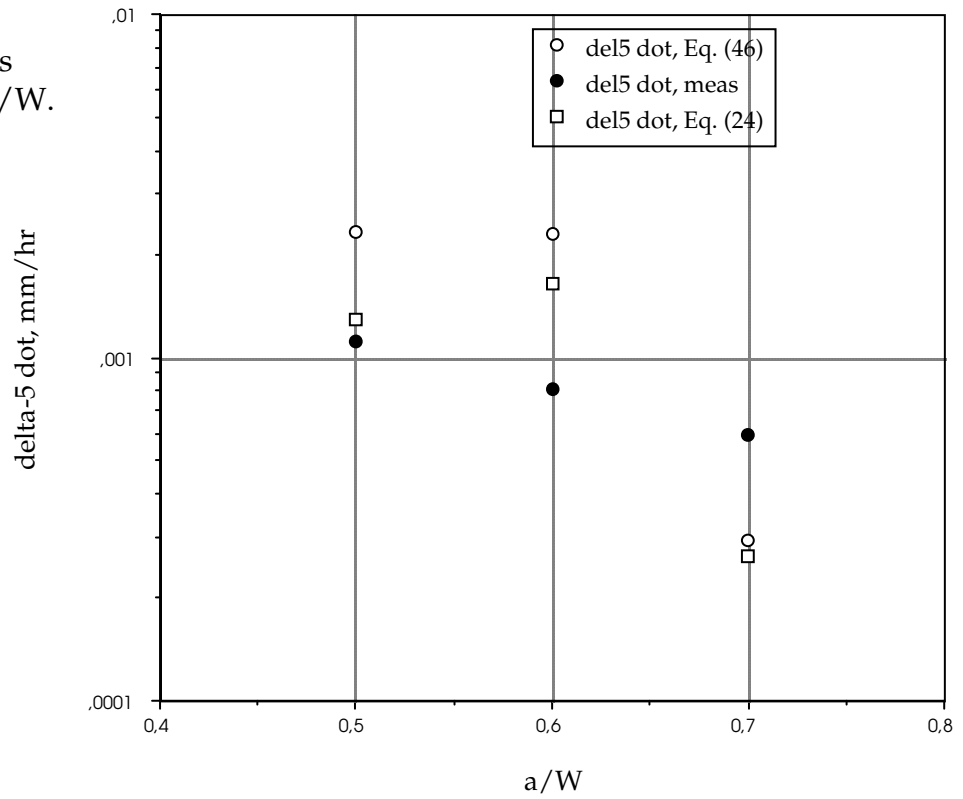

Figure 23:
Evaluation of C*
Parameters.

From the results shown in Figs. 20 and 23 it appears that the estimations are influenced by a/W. To look at this some results for a range of a/W ratios, $\dot{\delta}_5$ and C* values were analyzed for the deformation rate of 5 μm/hr as a function of a/W. The results are given in Figure 24 for the effect of a/W on $\dot{\delta}_5$ and in Figure 25 for the effect of a/W on C*. Here only the estimation of Eqs. (55) and (46) were used for $\dot{\delta}_5$ and the handbook formula of Eq. (56) for C*. Although the measured values for both parameters decrease steadily with a/W, the estimated values are not so orderly. They appear to fall in a somewhat irregular pattern. The estimated values become

low for a/W of 0.7. With additional test results and numerical analysis this trend can be re-evaluated.

Figure 24:
Delta-5 dot values as a function of a/W.

Figure 25:
C* as a function of a/W.
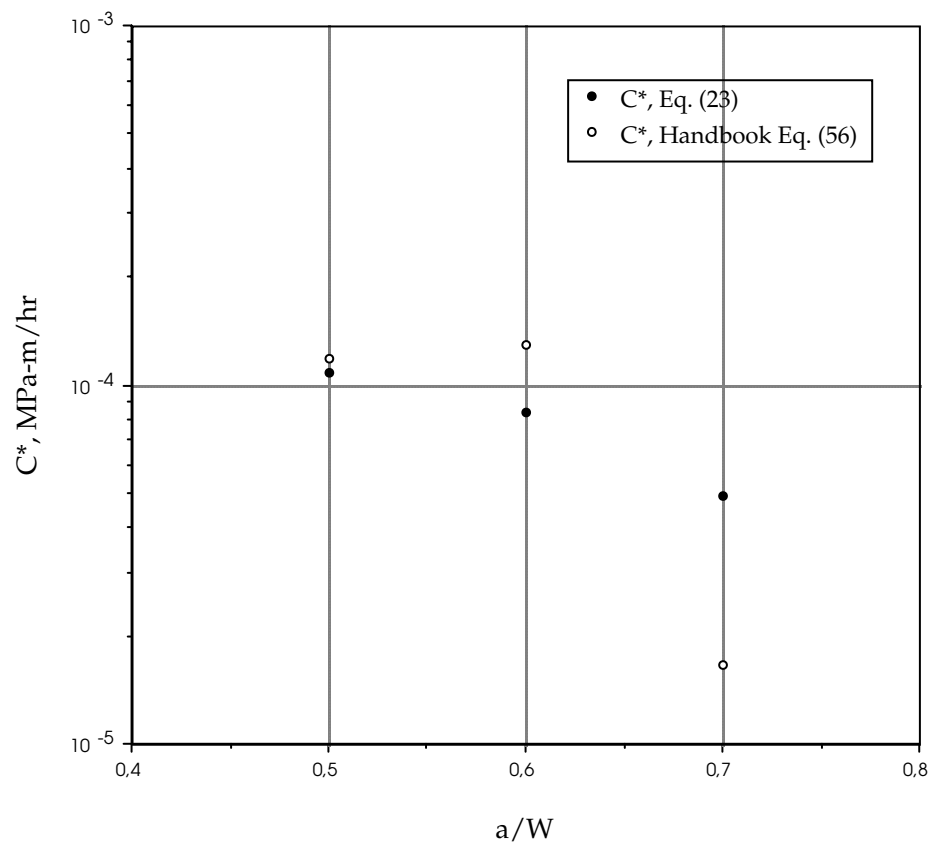
14 SUMMARY

Some forms for the creep crack extension characterizing parameters have been developed in this report. They are based on the assumption that the relationship between the force, crack length and deformation parameters has a separated format that is common for of all types of deformation. The separated format which needs to be experimentally or numerically verified, allows parameters for creep deformation to be derived from formats used in elastic and plastic deformation. These forms were used to look at the formats for parameters, C^* and C_t and to suggest new ones for the δ_5 based parameter based on a rate of change of that parameter, $\dot{\delta}_5$. These parameters are used to test for measuring creep crack extension rates and also for an engineering flaw assessment method for creep.

Experimental results from creep deformation tests conducted at 150 °C on a Mg-A31 alloy were used to evaluate these proposed formulations for creep deformation parameters. The primary evaluation was made on the form of the relationship between force, deformation rate and crack length. If this form exhibits separation, as does elastic and plastic deformation, then the equations used for plasticity can be used in evaluating the creep deformation parameters. This was shown to be essentially correct for the results analyzed here. The separation seems to work and the form of the crack length function is the same for creep as it is for plasticity. The evaluation of specific estimation forms for the $\dot{\delta}_5$ based parameters and the C^* parameters looked promising but not enough experimental results exist to give final conclusions about which forms are best. More experiments and finite element analyses are in progress and additional information on these forms will be available to further evaluate these formats.

REFERENCES

[1] Landes, J. D. and Schwalbe, K-H. "EFAM ETM-Creep 03 – The Engineering Flaw Assessment Method for Creep", GKSS 2002/23, GKSS-Forschungszentrum, Geesthacht.

[2] Landes, J. D. and Begley, J. A., "A Fracture Mechanics Approach to Creep Crack Growth". In: Mechanics of Crack Growth, ASTM STP 590, American Society for Testing and Materials, 1976, pp. 128–148.

[3] Nibkin, K. M., Webster, G. A. and Turner, C. E., Relevance of Nonlinear Fracture Mechanics to Creep Crack Growth". In: Cracks and Fracture ASTM STP 601, American Society for Testing and Materials, 1976, pp. 47–62.

[4] Saxena, A., "Creep Crack Growth Under Nonsteady-State Conditions". In: Fracture Mechanics Seventeenth Volume, ASTM STP 905, American Society for Testing and Materials, 1986, pp. 185•201.

[5] Schwalbe, K.-H., The Engineering Flaw Assessment Method ((EFAM) – Document EFM 96, GKSS 98/E/40, GKSS-Forschungszentrum, Geesthacht.

[6] Hellman, D and Schwalbe, K.-H., "On the Experimental Determination of CTOD Based R-Curves". In: The Crack Tip Opening Displacement in Elastic-Plastic Fracture Mechanics, Ed., K.-H. Schwalbe, Springer-Verlag, Heidelberg, 1986.

[7] Schwalbe, K.-H. and Cornec, A., "The Engineering Treatment Model (ETM) and its Practical Application. In: Fatigue and Fracture of Engineering Materials and Structures; Vol. 14, pp. 405–412, 1991.

[8] Schwalbe, K.-H. and Landes, J. D. "EFAM GTP-Creep 02 The GKSS test procedure for determining the creep crack extension of materials", GKSS 2002/22, GKSS-Forschungszentrum, Geesthacht.

[9] Ernst, H. A., Paris, P. C, Rossow, M., and Hutchinson, J. W., 1979, "Analysis of Load-Displacement Relationships to Determine J-R Curve and Tearing Instability Material Properties". In: Fracture Mechanics, ASTM STP 677, C. W. Smith, Ed., pp. 581–599.

[10] Ernst, H. A., Paris, P. C, and Landes, J. D., 1981, "Estimations on J-Integral and Tearing Modulus T from a Single Specimen Test Record". In: Fracture Mechanics: Thirteenth Conference, ASTM STP 743, Richard Roberts, Ed., pp. 476–502.

[11] Rice, J. R., Paris, P. C, and Merkle, J. G., "Some further results on J integral analysis and estimates". In: Progress in Flaw Assessment and Toughness Testing, ASTM STP 536, American Society for Testing and Materials, 1973, pp. 231–244.

[12] Ernst, H. A. and Paris, P. C., "Techniques of analysis of load-displacement records by J integral methods", Nuclear Regulartory Commission, NUREG/CR.1222, Jan. 1980.

[13] Sharobeam, M. H. and Landes, J. D., "The Load Separation Criterion and Methodology in Ductile Fracture Mechanics". In: International Journal of Fracture, Vol. 47, 1991, pp 81–104

[14] Donoso, J. R. and Landes, J. D., "A Unifying Principle for Evaluating Fracture Toughness in the Elastic and Plastic Regimes with Planar Fracture Specimens". In: Fatigue and Fracture Mechanics: 30th Volume, ASTM STP 1360, P. C. Paris and K. L. Jerina, Eds., American Society for Testing and Materials, West Conshohocken, PA, 2000, pp. 36–53.

[15] ASTM E 1820, "Standard Test Method for Measurement of Fracture Toughness". In: ASTM, Annual Book of Standards, Vol. 03.01.

[16] Donoso, J. R. and Landes, J. D., "Common Format Equation Approach for Developing Calibration Curves for Two-Dimensional Fracture Specimens from Tensile Data". In: Engineering Fracture Mechanics, Vol. 54, No. 4, 1996, pp. 499–512

[17] Donoso, J. R. and Landes, J. D., "Advantages of the Concise K and Compliance Formats in Fracture Mechanics Calculations". In: Fatigue and Fracture Mechanics, 32nd Volume, ASTM STP 1406, R. Chona, ed., American Society for Testing and Materials, West Conshohocken, PA, 2000, pp. 261–278.

[18] Saxena, A. Nonlinear Fracture Mechanics for Engineers, CRC Press, Boca Raton, FL, 1998.

[19] Riedel, H. and Rice, J. R., "Tensile Cracks in Creeping Solids". In: Fracture Mechanics Twelfth Conference, ASTM STP 700, American Society for Testing and Materials, 1980, pp. 112–130.

[20] Tada, H., Paris, P. C. and Irwin, G. R., "The Stress Analysis of Cracks Handbook," third edition, American Society of Mechanical Engineers, New York, NY, 2000.

[21] Braga, L. M., "The application of the Engineering Treatment Model (ETM) to creep crack growth, GKSS Technical Note GKSS/WW/93/8, August, 1993.

[22] Saxena, A., Dogan, B., and Schwalbe, K-H., "Evaluation of the relationship between C^*, δ_5, and δ_τ during creep crack growth". In: Fracture Mechanics: Twenty-Fourth Volume, ASTM STP 1207, J. D. Landes, D. E. McCabe and J. A. M. Boulet, Eds., ASTM, 1994, pp. 510–526.

[23] Schwalbe, K.-H., Zerbst, U., Kim, Y.-J., Brocks, W., Cornec, A., Heerens, J. and Amstutz, H., "EFAM ETM 97 The ETM Method for Assessing the Significance of Crack-like Defects in Engineering Structures, Comprising the Versions, ETM 97/1 and ETM 97/2", GKSS 98/E/6, GKSS-Forschungszentrum, Geesthacht.

[24] Bassani, J. L., Hawk, D. E. and Saxena, A., " Evaluation of the C_t Parameter for Characterizing Creep Crack Growth in the Transient Regime". In: Nonlinear Fracture Mechanics: Time Dependent Fracture Mechanics, Vol. 1, ASTM STP 995, American Society for Testing and Materials, 1976, pp. 47–62.

[25] Kumar, V., German, M. D., and Shih, C. F., "An Engineering Approach for Elastic-Plastic Fracture Analysis," NP 1931, EPRI Project 1237-1, July 1981.

[26] R-5, "Assessment Procedure for the High Temperature Response of Structures", Issue 2, April, 1996.